2006-08-16

Feedback Applications in Active Noise Control for Small Axial Cooling Fans

Matthew J. Green
Brigham Young University - Provo

FEEDBACK APPLICATIONS IN ACTIVE NOISE CONTROL FOR SMALL AXIAL COOLING FANS

by

Matthew J. Green

A thesis submitted to the faculty of

Brigham Young University

in partial fulfillment of the requirements for the degree of

Master of Science

Department of Physics and Astronomy

Brigham Young University

August 2006

BRIGHAM YOUNG UNIVERSITY

GRADUATE COMMITTEE APPROVAL

of a thesis submitted by

Matthew J. Green

This thesis has been read by each member of the following graduate committee and by majority vote has been found to be satisfactory.

Date	**Scott D. Sommerfeldt, Chair**
Date	**Timothy W. Leishman**
Date	**Randal W. Beard**

BRIGHAM YOUNG UNIVERSITY

As chair of this candidate's graduate committee, I have read the thesis of Matthew J. Green in its final form and have found that (1) its format, citations, and bibliographical style are consistent and acceptable and fulfill university and department style requirements; (2) its illustrative materials including figures, tables, and charts are in place; and (3) the final manuscript is satisfactory to the graduate committee and is ready for submission to the university library.

_____ _____

Date **Scott D. Sommerfeldt**
Chair, Graduate Committee

Accepted for the Department

_____

Ross L. Spencer
Graduate Coordinator

Accepted for the College

_____

Thomas W. Sederberg, Associate Dean
College of Physical and Mathematical

ABSTRACT

FEEDBACK APPLICATIONS IN ACTIVE NOISE CONTROL

FOR SMALL AXIAL COOLING FANS

Matthew J. Green

Department of Physics and Astronomy

Master of Science

Feedback active noise control (ANC) has been applied as a means of attenuating broadband noise from a small axial cooling fan. Such fans are used to maintain thermal stability inside of computers, projectors, and other office equipment and home appliances. The type of low-level noise radiated from axial cooling fans has been classified as harmful to productivity and human well being.

Previous research has successfully implemented feed-forward ANC, targeting specific narrow-band fan noise content related to the blade passage frequency (BPF) of the fan. The reference signal required for a feed-forward algorithm limits its ability to attenuate much of the noise content; however, it is also desirable to reduce broadband fan noise. Feedback control is a logical alternative in the absence of a valid reference signal.

The fan used for this research was mounted in one of the six aluminum panels that constituted a mock computer case. The fan was surrounded by four miniature loudspeakers as control sources and four small electret microphones as error sensors. A feasibility study was conducted with a single channel of analog feedback control. However, for the majority of this research, the ANC algorithm was executed on a digital signal processor. Several electronic modules provided the necessary signal conditioning and conversion for the process.

A method is proposed and validated for predicting the overall attenuation that can be obtained for a specific fan, based on its autocorrelation measurement. Studies were performed in order to determine the difference in performance between static and adaptive controllers. Comparisons are made between decentralized and centralized controllers, the results of which are presented in this thesis.

Feedback ANC is demonstrated as a good alternative to feed-forward ANC for the reduction of BPF related tonal fan noise content. Some low-frequency broadband attenuation is achieved. The delay time associated with current DSP technology is shown to be too long to effectively attenuate flow noise (the main component of broadband fan noise). Adaptive control proved to be necessary for stability and performance in the feedback controller. Decentralized control is shown to outperform centralized control for this specific application.

ACKNOWLEDGEMENTS

I would like to express my gratitude to the following people for support and guidance through the process of researching for and writing this thesis:

- Scott Sommerfeldt, my advisor, for making his time and experience available to me and inspiring me to become an expert in my field;
- Timothy Leishman, for serving on my committee, supporting me with good literature, and teaching acoustics with passion;
- Randal Beard, for serving on my committee, providing my introduction to feedback control, and encouraging me to think thoroughly;
- Kent Gee and Brian Monson for paving the way for successful fan noise control at BYU and for supportive encouragement;
- Connor Duke, Cole Duke, and Brent Hicks for tremendous help with hardware assembly and measurements;
- Nan Ellen Ah You and Diann Sorensen for kind and helpful administration of all graduate school and thesis procedures;
- BYU Acoustics Research Group for contributing support and excitement to the research and coursework done in Acoustics at BYU;
- Ron, Sheila, Denise, Lori, and Amanda Green for love, preparation, and encouragement;
- Kristen, Allyson, and Emily Green for inspiring me and partnering with me in all aspects of life and making this work fun and meaningful.

TABLE OF CONTENTS

LIST OF FIGURES

CHAPTER 1

INTRODUCTION

1.1 Active Noise Control

The first active noise control (ANC) patent was filed by P. Lueg in 1936. Lueg's experimental work in noise control was largely unsuccessful due to problems he faced with instability.[1] ANC experiments were further explored in the 1950's. Olson and May implemented their so-called electric sound absorber as a "spot sound reducer".[2] Many early attempts to suppress noise relied on the superposition of waves inside of a tube or duct, and were realized by analog feedback or feed-forward control. Advancements in the performance and stability of ANC systems did not surface until more recent years with the development of digital signal processing (DSP) hardware. Digital electronics allow for stable implementations of very complex control systems that are unrealizable with analog hardware. Digital signal processing has led to the development of new algorithms for control with increased capabilities.

Improvements have also been made in the physical implementation of ANC systems. Hardware arrangements that incorporate the effects of strong source coupling in addition to wave superposition provide a more effective and global control of noise that does not rely on the noise source being constrained by a duct. ANC systems with multiple control channels can improve the amount of source coupling and therefore achieve greater overall noise reduction. Assuming that the strength of a source is proportional to the size of its radiating surface, the size of secondary source needed to produce the desired output for a given primary source decreases as additional secondary sources are introduced. Decreased secondary source size allows for closer proximity

between the primary and secondary sources. This provides stronger source coupling at a given frequency.

To date, ANC systems have been successfully implemented in headsets, HVAC systems, aircraft, automobiles, and other applications.

1.2 Fan Noise

Axial cooling fans like those found in computers, projectors, and other electronic devices are major contributors to the overall noise level in a home or office area. Exposure to low level noise has been shown to have negative effects on work performance as well as psychological health. Those exposed to office noise are not only consciously annoyed, but become less likely to attempt difficult tasks without recognizing it. Disturbances from uncontrollable sources cause a person to become less likely to comfort themselves in situations where they have control to do so.[3]

Each piece of electronic equipment in an office is often accompanied by one or more small axial cooling fans in order to keep the internal electronics at a desirable operating temperature. Since much of the noise generated by office equipment is due to these fans, the control of noise from small axial cooling fans has been the topic of recent research.

The noise produced by an axial fan is dominated by harmonic tones related to the blade passage frequency (BPF). There typically exist additional smaller tones related to the fan motor speed or due to flow restrictions. Also, the flow of the fan creates a broadband noise floor. The sources of axial fan noise are discussed in more detail in

Section 2.1 of this thesis. Figure 1.1 shows the auto power spectrum of a typical 60 mm axial cooling fan.

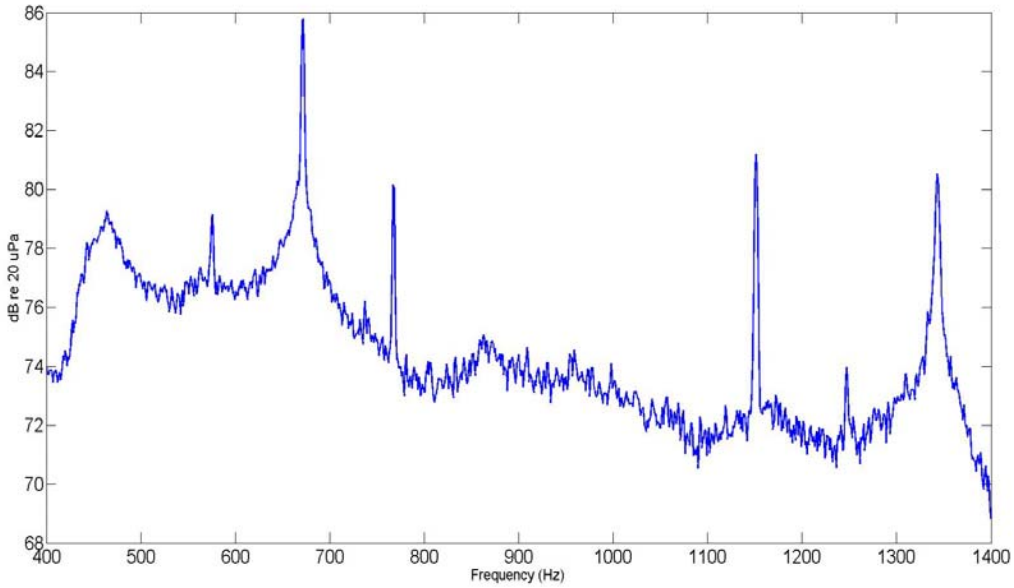

Figure 1.1 Auto power spectrum of a 60 mm axial cooling fan.

Most of the radiated sound power occurs at frequencies lower than 2 kHz. Since the source of the noise is relatively small compared to the wavelength of the noise, it is well suited for active noise control.

1.3 Previous Fan ANC Systems

Several attempts have been made to reduce the level of noise produced by cooling fans. Each ANC attempt has had varying levels of success. Lauchle, *et al*. attenuated tonal fan noise by using the vibrationally actuated fan itself as the secondary source for ANC.[4] This method provided substantial attenuation of BPF and the second harmonic of BPF, but no attenuation of higher harmonics. Kenji, *et al*. combined active and passive control methods by mounting a computer fan in a short passively-lined duct and applying

a broadband feedback controller.[5] The performance of such a system is desirable. However, it is not feasible to attach a duct to the cooling fans of typical office equipment. Quinlan reduced tonal noise from an axial cooling fan by placing a loudspeaker next to the fan on a baffle.[6] Gee and Sommerfeldt improved on the performance and practicality achieved by Quinlan through a multichannel implementation of the filtered-x least mean squares (FXLMS) algorithm with near-field error sensors.[7] Global attenuation of tonal noise was achieved in the far field to the degree that the BPF and three of its harmonics were attenuated to the broadband noise floor. The single channel FXLMS algorithm is depicted in the block diagram of Figure 1.2. The system components in this and other block diagrams in this thesis are all Z-transform representations of the system elements. The Z-transform converts a discrete real-time domain signal into a complex frequency domain signal.[8]

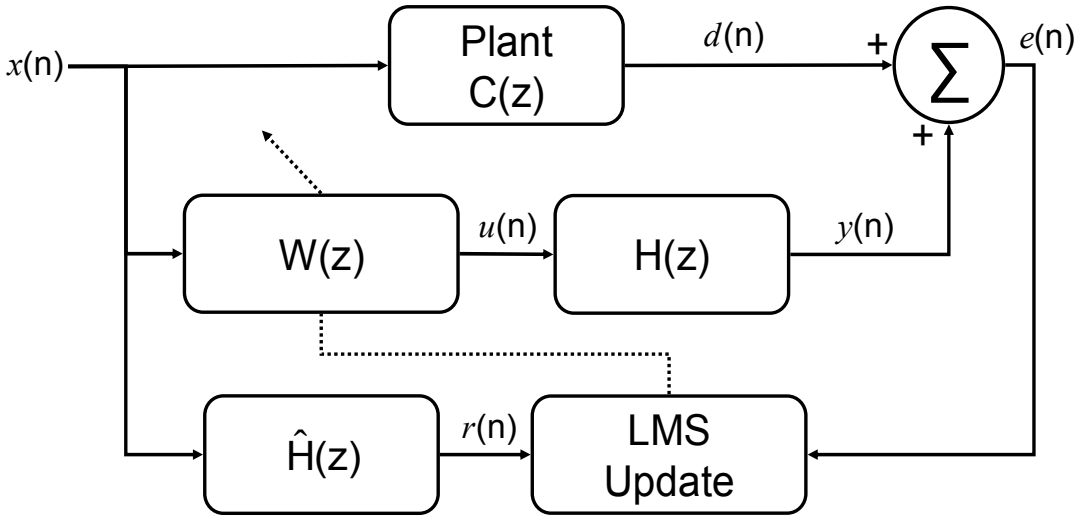

Figure 1.2 Block diagram of the filtered-x least mean squares algorithm.

A filtered-x algorithm, rather than the standard LMS algorithm, becomes necessary for ANC or any application where the signal path is at least partially acoustical.

The standard LMS algorithm requires that the path between the output of the DSP and the input of the DSP be negligible for stability. An active noise control system incorporates the acoustical summation of the primary noise signal with the control signal in order to produce the error signal, *e(n)*. The acoustical delay associated with this summation, the response of the transducers, and the signal conditioning devices are combined to form the so called secondary path, *H(z)*. The secondary path is inserted after the control filter in the block diagram so that its effects are considered when calculating the output signal, *y(n)*. Since the response of the secondary path is unknown, an estimation of H(z) is obtained by an off-line system identification routine, which measures the impulse response of the secondary path. The secondary path estimation is used to produce the filtered-x signal, *r(n)*, which is used for the LMS update.

The success of the above-mentioned tonal noise control is largely due to two discoveries related to the number of control sources used for optimum control and the ideal placement of near-field error sensors which result in global control of noise.

The use of multiple control sources can allow for each of the sources to be smaller in size as was described in Section 1.1 of this thesis. Smaller control sources can be placed physically closer to the primary noise source. Thus, the amount of source coupling is increased and the radiation efficiency of the total system is decreased. It has been theoretically and experimentally shown that the amount of global noise reduction improves with an increased number of control sources. However, improvements become insignificant beyond the use of three or four control sources.[7] A comparison of ideal theoretical reductions is presented as a function of *kd* (the wave number times the

distance between the primary and secondary sources) in Figure 1.3.[7,9] All sources are assumed to radiate as monopoles.

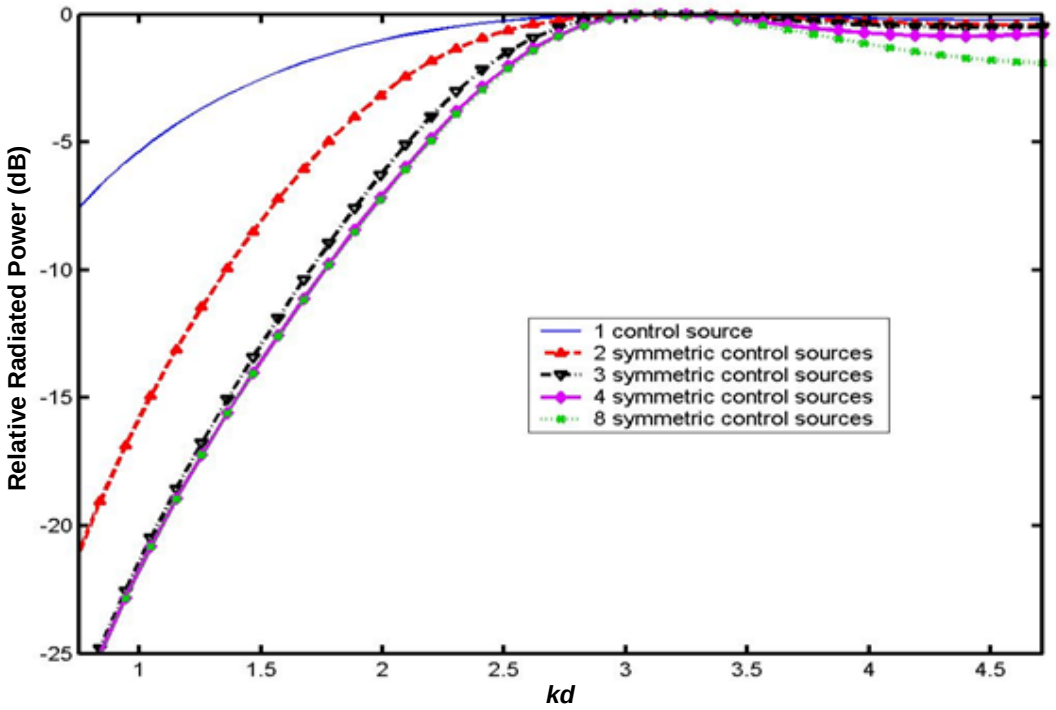

Figure 1.3 Radiation power of multiple control source configurations relative to that of a monopole source.

In order for the ANC of cooling fan noise to be commercially viable, the solution must not include the placement of any hardware in the far-field of the fan. Conventional wisdom has considered the placement of error sensors in the near-field of the primary and secondary sources to be an unwise practice.[10] When squared acoustic pressure is minimized at a randomly chosen point in the near-field of a noise source it cannot necessarily be determined what will happen in the far-field. The far-field squared pressure might be globally attenuated, or it might be attenuated in some places and increased in others. However, the existence of specific near-field error sensor locations which result in global far-field squared pressure reduction has been demonstrated. These positions exist where the acoustic pressure attenuation is greatest when the control

sources produce an output which minimizes the total radiated power of the system. The source strength to minimize the total radiated power from two sources is described by

$$\mathrm{Q_s} = -\left|\mathrm{Q}_p\right| \times \frac{\sin(kd)}{kd}, \tag{1.1}$$

where $\mathrm{Q_p}$ is the strength of the primary source, $\mathrm{Q_s}$ is the strength of the secondary source, k is the acoustic wave number, and d is the distance between the two sources.

This equation can be expanded for multiple primary or secondary sources. This is shown for a single primary source and four secondary sources as follows.

$$\overline{\mathrm{Q}}_\mathrm{s} = -\overline{A}^{-1}\overline{B}\,, \tag{1.2}$$

$$\begin{aligned} \overline{A} &= \frac{1}{2}\mathrm{Re}\left[\overline{Z}_{ss}\right], \\ \overline{B} &= \frac{1}{2}\mathrm{Re}\left[\overline{Z}_{sp}\right] \times \mathrm{Q}_p\,, \end{aligned} \tag{1.3}$$

$$\mathrm{Re}\left[\overline{Z}_{ss}\right] = \begin{bmatrix} Z_{s1s1} & Z_{s1s2} & Z_{s1s3} & Z_{s1s4} \\ Z_{s2s1} & Z_{s2s2} & Z_{s2s3} & Z_{s2s4} \\ Z_{s3s1} & Z_{s3s2} & Z_{s3s3} & Z_{s3s4} \\ Z_{s4s1} & Z_{s4s2} & Z_{s4s3} & Z_{s4s4} \end{bmatrix}, \mathrm{Re}\left[\overline{Z}_{sp}\right] = \begin{bmatrix} Z_{s1p} \\ Z_{s2p} \\ Z_{s3p} \\ Z_{s4p} \end{bmatrix}. \tag{1.4}$$

The over-score represents matrix notation and Z represents acoustic impedance. The subscripts p and s denote whether the source or impedance is for a primary or secondary source. The number following a subscripted letter specifies which of the multiple sources of that type is being referenced. The absence of a number following a subscripted letter denotes that there is only one of that particular type of source.

For any two sources *a* and *b*, the self or mutual impedance associated with the sources is calculated as

$$\mathrm{Re}[Z_{ab}] = \frac{k^2 \rho_0 c}{4\pi} \times \frac{\sin(kd_{ab})}{kd_{ab}}, \qquad (1.5)$$

where for a self impedance, $a = b$. The variable, k, represents the acoustic wavenumber, c is the speed of sound in air, ρ_0 is the characteristic impedance of air, and d_{ab} is the distance between sources *a* and *b*.

The near-field in-plane pressure is illustrated in Figure 1.4 for a point monopole primary noise source being controlled by four point monopole secondary sources at 800 Hz, where the spacing between the primary source and each secondary source is 56 mm.

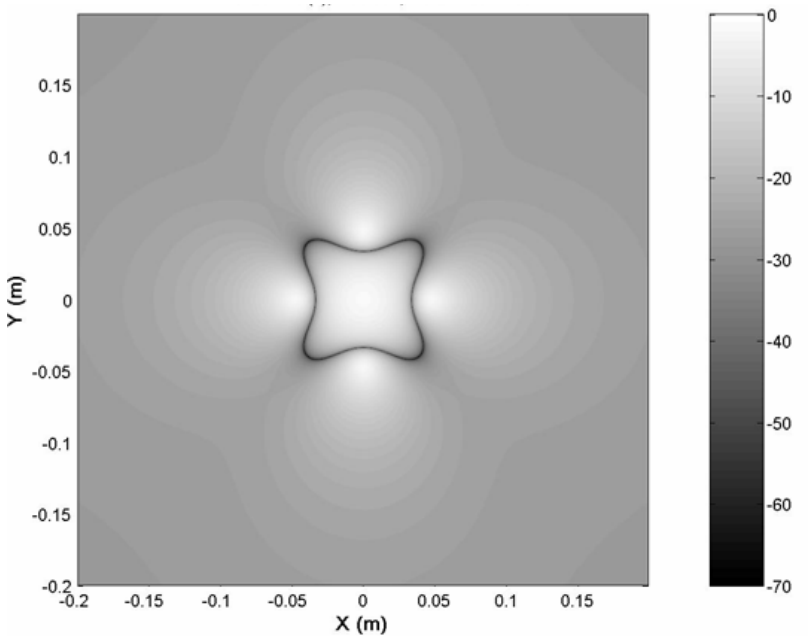

Figure 1.4 Near-field pressure attenuation (in dB) for a point monopole noise source controlled by four point monopole secondary sources operating at 800 Hz.

1.4 Feedback ANC

A feed forward ANC system is typically desirable in applications where a sufficiently coherent reference signal can be obtained. Under circumstances where such a reference signal is not available, the error signal (output of the open-loop system) is fed back to the controller so that the primary noise can be estimated. Thus, for fan noise, a feedback system is capable of controlling some noise that feed forward systems are incapable of controlling unless the fan is mounted in a duct. The cost of such flexibility comes in the form of decreased performance, for most applications, and increased likelihood of instability. However, there exist some control situations where the secondary path delay is sufficiently low, and feedback control will perform more favorably than feed forward control.[11]

The time delay introduced by the feedback path decreases coherence between the error signal and the estimated reference signal. Noise must be correlated with itself at some time greater than the total group delay of the control system in order to be controlled by feedback. Also, since the estimation of the primary noise is formulated from the error signal it includes not only the primary noise but unwanted content present either electrically or acoustically at the error sensor. In spite of these drawbacks, feedback ANC has been shown to successfully reduce unwanted noise in several applications.[12]

The reference signal used for feed forward ANC of tonal fan noise is a non-acoustical signal such as the fan's tachometer output or the pulses from an emitter detector pair. These reference signals are incapable of detecting broadband noise. It

follows logically that feedback ANC should be used in order to attenuate the broadband noise of a fan.

1.5 Research Overview

With prior success in the control of BPF related fan noise in a free-radiating environment, it becomes desirable to reduce the broadband component of the fan noise as well. An ANC system for a small cooling fan that could obtain any significant reduction of flow noise in addition to tonal reduction would cause office equipment fans to be reclassified from quiet annoyances to virtually unnoticeable. Unlike feed-forward ANC systems previously used for fans, a broadband ANC system would provide cancellation of tonal noise that is unrelated to the BPF.

This research was motivated by a desire to discover the possibilities and limitations of broadband feedback ANC as a viable replacement for or addition to previous fan ANC methods, with the specific goal of reducing broadband fan noise. Benefits from a successful broadband ANC system would include improved fan noise reduction, elimination of the hardware needed for a non-acoustical reference signal, and more flexibility in the type of noise attenuated by the controller.

A simple analog controller was applied to an axial cooling fan in order to verify the feasibility of global broadband control. Static and adaptive controllers were designed and implemented on a digital signal processor and tested for performance, stability, and flexibility. The behavioral differences between centralized and decentralized controllers were evaluated, and the possibility of a partially centralized controller reviewed. Feed-

forward and feedback controllers were combined in a hybrid system in an attempt to reap the benefits of both forms of control.

1.6 Thesis Organization

The noise emitted by small axial cooling fans will be characterized in Chapter 2 of this thesis. The ability to control the fan noise will also be discussed. The use of feedback control as a means of noise suppression will be defined in Chapter 3. This chapter will likewise include an exploration of feedback algorithm development and various system configurations. These include discussions on stability, causality, analog and digital implementation, internal model control, adaptive control, decentralized and centralized controllers, and feed-forward/feedback hybrid control. The experimental apparatuses will be presented in Chapter 4 along with descriptions of the hardware used and measurements taken. Chapter 5 contains the results from the experimental data collected for this thesis. Chapter 6 presents conclusions drawn from the theoretical background given in Chapters 2 and 3 as well as the experimental results from Chapter 5.

CHAPTER 2

NATURE OF AND ABILITY TO CONTROL FAN NOISE

2.1 Fan Noise

Aerodynamic interaction between fan impeller blades and downstream struts causes tonal noise to be generated at the BPF and as well as at harmonics of the BPF.[13] Random fluctuations in blade loading lead to the creation of broadband noise radiation.[14] Noise is also generated from motor vibration and other sources that are more specifically influenced by the manner in which a fan is mounted and mechanically loaded. A well balanced, structurally isolated fan will typically radiate only a set of BPF related tones and a broadband noise floor.

2.2 Autocorrelation

The ability to control noise by means of feedback ANC can be determined from the autocorrelation of the noise. Correlation is a statistical measure of the similarities between two sets of data or signals. Autocorrelation evaluates the correlation of a signal against a time shifted version of itself. The discrete autocorrelation function is written as

$$R_i = \sum_{j=0}^{N-1} a_j a_{j+i} \,, \tag{2.1}$$

where R_i is the amount of correlation between the signal a and a version of a shifted i discrete samples in time.

2.3 Group Delay

A feedback control system will have a group delay associated with it. Often, the greatest contribution to the delay will be the acoustical propagation delay of the secondary path, or path between the control sources and the error sensors. The calculation of this delay is given by

$$Acoustic\ Delay = \frac{d_{ps}}{c}, \tag{2.2}$$

where c is the speed of sound in the medium between the two devices and d_{ps} is the distance between the two devices.

The phase shift associated with filtering also increases group delay in a control system. Filters are needed for stability and performance in a feedback system. The amount of delay from filtering varies with filter type, order, and cutoff frequency. Other forms of delay include electrical propagation delay, transducer response time, data converter delay, and DSP computation time. These sources of delay are more difficult to compute and typically contribute less to the total group delay than the first two types of delay mentioned. Total group delay can be measured by observing the delay time associated with the impulse response of the complete secondary path.

2.4 Control Prediction

Noise reduction should be attainable by means of feedback ANC provided that the noise is correlated with itself at a time greater than the group delay of the control system. "A long control filter will thus cancel all the predictable components of the disturbance, leaving only that part which is uncorrelated from one sample to the next, which is white

noise."[11] With an understanding that feedback controllers take advantage of the predictability of the disturbance over the timescale of the group delay in order to achieve control, it is reasonable to assume that the amount of attainable control for a given feedback ANC system may be quantified by knowing how much of the disturbance is correlated with itself at a time greater than the group delay. Let E_p represent the highest single level of the magnitude of the autocorrelation function present after time t_g (group delay time). E_{total} is the autocorrelation level at zero delay. This value will be one for a normalized autocorrelation function. The theoretical maximum amount of attainable control of a noise source can be calculated as

$$Attenuation(dB) = -10 \times \log\left(1 - \frac{E_p}{E_{total}}\right), \qquad (2.3)$$

which was created by the author of this thesis and is based on the writings of Stephen Elliott that were referenced earlier in this paragraph. Equation 2.3 was verified experimentally as a part of this thesis research and used to predict the outcome for systems that, to date, have not been realized.

Figure 2.1 shows the normalized autocorrelation function for the 60 mm axial cooling fan used in this research.

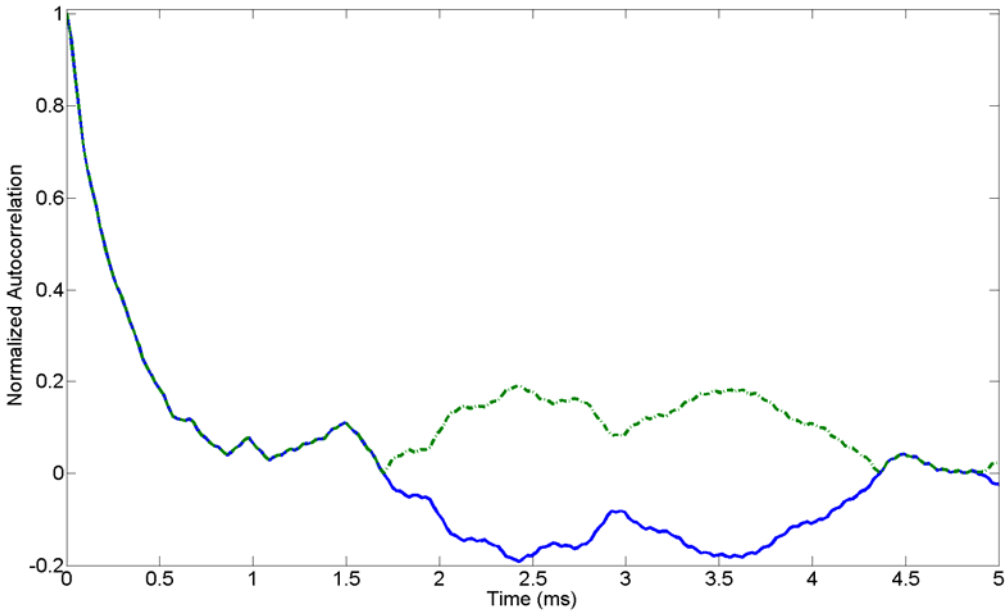

Figure 2.1 Normalized autocorrelation measurement of a 60 mm axial cooling fan (absolute value shown as green dotted line).

The level of autocorrelation of the fan noise decreases as time increases, but there exist areas of increased correlation as the time shift brings periodic components of the fan noise in and out of phase. Harmonic content that is time aligned in phase with itself is positively correlated, while harmonic content that is time aligned out of phase with itself is negatively correlated. For the purpose of attenuation prediction it matters only that the noise be correlated and the sign associated with the correlation is unimportant. Figure 2.2 shows the theoretical level of attenuation possible for the 60 mm axial cooling fan as a function of group delay.

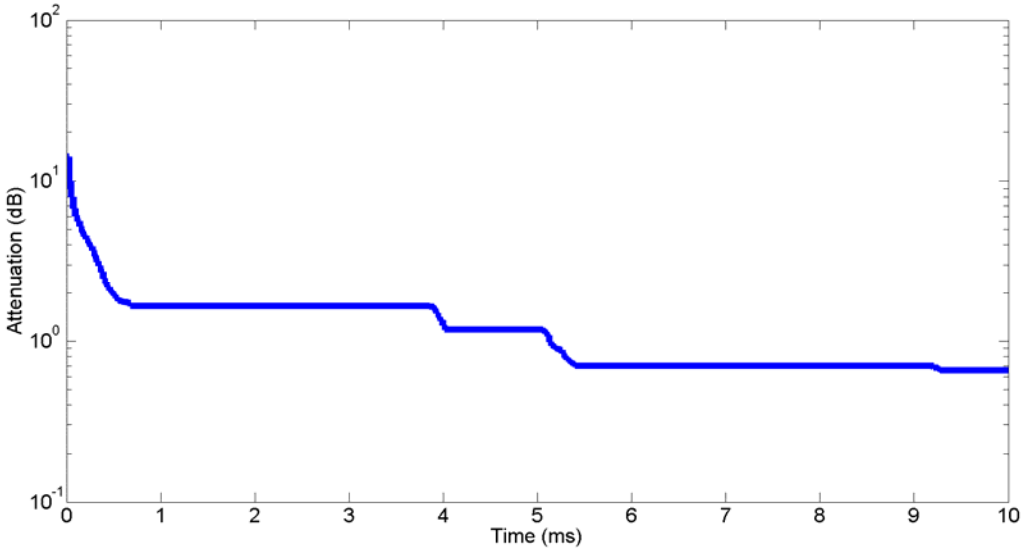

Figure 2.2 Predicted attenuation in dB vs. group delay based on autocorrelation measurement of a 60 mm axial cooling fan.

Due to the definition of E_p, the function of possible attenuation can never increase with increased group delay. Also, after group delay has reached a certain point, the change in possible attenuation becomes stepped rather than continuously changed. This transition occurs when the group delay corresponds to the lowest point on the main lobe of the autocorrelation function that is still greater than any other point to the right. This transformation from a more continuous function to a stepped function identifies a benchmark for the group delay of a control system that is designed for broadband noise reduction. A system with a group delay falling in the stepped region of this function will primarily be successful at reducing only tonal content in noise, while a system with a group delay less than the benchmark will successfully reduce the broadband content of the broadband noise as well. Thus, the minimization of group delay for a feedback ANC system is critical.

CHAPTER 3

FEEDBACK CONTROL

3.1 Use and Definition

"Control is the process of making a system adhere to a particular value, called the reference value." "In closed-loop control the system includes a sensor to measure the output and uses feedback of the sensed value to influence the control variable."[15] An idealistic representation of this process is illustrated in Figure 3.1 as it applies to fan noise control. The goal of this system is to minimize the mean square of the error signal, *e(n)*, where *e(n)* is the acoustical summation of the fan noise (or disturbance signal) *d(n)* and the system output, *y(n)*. The signal *y(n)* is produced as the result of the error signal being filtered by the controller, *W(z)* and the plant, *H(z)*. The plant, or system to be controlled, includes any electrical, mechanical, or acoustical response of the physical system.

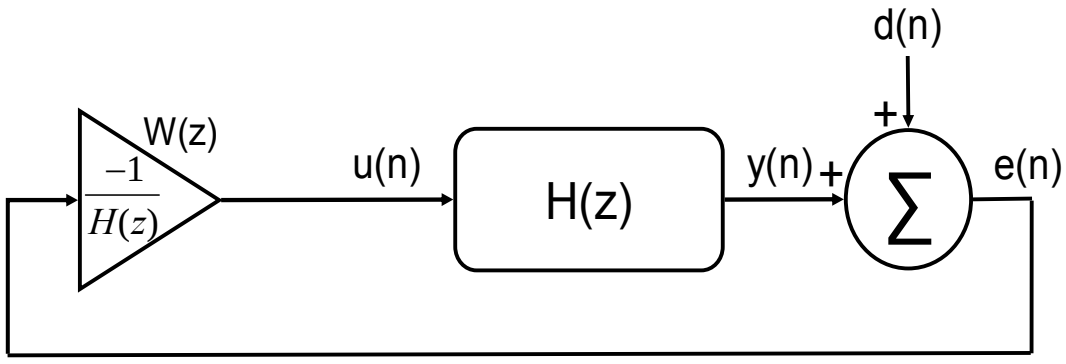

Figure 3.1 Block diagram of implementation of an ideal feedback control system.

3.2 Stability

Stability for systems involving feedback is determined by the Nyquist Stability Criterion, which states that the overall phase of the open loop system response must be

greater than -180 degrees at unity gain.[16] The fulfillment of this criterion guarantees a finite output for the closed loop system by insuring that the system is a negative feedback system. In practice, stability for feedback systems is achieved by filtering the output of the sensor and shaping the frequency response of the controller. Realistically speaking, the Nyquist Stability Criterion should be met and exceeded by a generous margin.

Margins of stability are separated into two types: gain margin and phase margin. Gain margin is the additional tolerable amount of gain increase for a system that is to remain stable, and is given in dB. Phase margin is the additional tolerable phase shift in the plant for a system that is to remain stable, and is given in degrees. Stability is best ensured by certainty of the plant response. An accurate model of the plant will allow for aggressive controller design with a high probability of stability. Any uncertainty in the plant response will result in either the need to increase gain and phase margins at the cost of control performance or greatly increase the risk of instability.

3.3 Causality

When the outputs and internal states of a system depend only on past and current inputs, that system is causal.[17] All systems that are to be physically realized must be causal systems. While designing a controller to provide the ideal output based on input from a sensor it will frequently become desirable to break the law of causality by obtaining future inputs in order to calculate the present output values. Depending on the type of system implementation, certain steps must be taken during the design process in order to guarantee causality.

3.4 Analog Implementation

The control filter, W(z), from Figure 3.1 is sometimes implemented with analog electronics. The transfer function of the controller can be written as a pole-zero equation of the form

$$W(z) = \frac{P(z)}{Q(z)}. \tag{3.1}$$

The vales where $P(z) = 0$ constitute the zeros of the system and the values where $Q(z) = 0$ constitute the poles of the system.

There exist analog circuit approximations for many common pole zero equations. If a pole zero equation has many roots, an appropriate analog circuit approximation becomes difficult or impossible to find. Typically, analog feedback controllers are simple RC circuits known as compensators. These compensators include elements for controlling overall gain, introducing phase leads or lags, and filtering out undesired frequency content.[18]

In practice, no feedback control system is entirely stable or unstable for all inputs. Each system will satisfy the Nyquist stability criterion for a certain frequency band of input signals. It is the goal of most designs to maximize that frequency band by keeping the phase and magnitude of the open loop system as flat as possible. Stability is then provided by filtering the disturbance signal such that it contains significant content only in the frequency range where the Nyquist stability criterion is met . If the system is incapable of responding well at frequencies where the gain or phase margins are unfavorable then positive feedback can be prevented. In this case, however, the solution is also part of the problem. The introduction of filters for stability will increase the phase

shift in the closed loop response, thus decreasing gain and phase margins. Careful consideration must be used in determining the type of filter to use for stability, the order of that filter, and where its cutoff frequency should be.

The group delay introduced by an analog controller is significantly less than the delay for a digital controller. This becomes increasingly important for systems with small propagation delays like that considered in this thesis, where the majority of the total group delay is due to filters and hardware rather than acoustical propagation time. Analog controllers are also generally less expensive and require less maintenance. Arguments against analog control are primarily focused on the lack of flexibility in and simplistic nature of the controllers. Systems requiring control beyond that provided by a first or second order filter can generally not be effectively compensated for by analog electronics. Implementations of controllers are only as precise as the tolerance of the circuit components will allow. Additionally, analog controllers lack the ability to do much real-time adaptation. For these reasons, analog control is best suited for fairly static environments with relatively simple plants.

A single channel analog controller was designed for this research. Analog control was used as a feasibility study for feedback control of the cooling fan noise, and was therefore kept simple. The signal from the error microphone was fed back to the control loudspeaker through an inverting amplifier and a single-pole, low-pass RC filter for stability and phase optimization. The cutoff frequency of the filter was near 1000 Hz. Potentiometers, rather than fixed resistors, were used for the filter as well as the gain stage. The potentiometer on the cutoff filter was adjusted until the phase shift of the closed loop system was optimal for feedback control. Next, the potentiometer on the gain

stage was adjusted until the maximum level of stable control was achieved. A schematic representation of the analog feedback control system is provided in Figure 3.2.

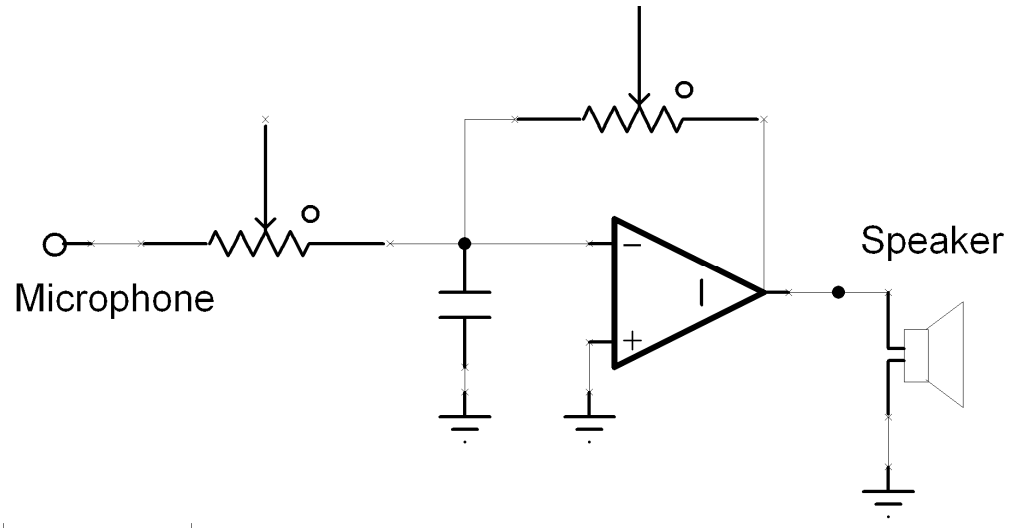

Figure 3.2 Schematic representation of the analog controller hardware used for this research.

3.5 Digital Implementation

ANC system controllers are most frequently implemented on digital hardware. Filters are created digitally either as infinite impulse response (IIR) systems or as finite impulse response (FIR) systems. The response of an IIR filter to an impulse is non-zero over an infinite interval of time. The practical creation of such a filter involves recursive iteration. The response of an FIR filter to an impulse is zero after a finite length of time. Real systems with infinite responses are approximated as FIR systems either through the use of truncation or windowing of the impulse response of the system. Control filters for ANC are designed as finite impulse response (FIR) filters and implemented on digital signal processors.[19] The controller, *W(z)*, becomes a vector of *N* FIR filter coefficients whose time response has the following form for any discrete time *n*,

$$W(z) = \sum_{n=0}^{N-1} \overline{w}(n)\, z^{-n}$$
$$\overline{w}(n) = \left[w_1(n)\ w_2(n) \ldots w_{N-2}(n)\ w_{N-1}(n) \right]. \qquad (3.2)$$

The filter length, *N*, is a finite number determined, in the case of broadband noise reduction, by the frequency bandwidth where attenuation is desired. As the number of filter coefficients (or taps) increases for a given control bandwidth so does the frequency resolution of the control system. The residual spectrum of the error signal will become more flat as *N* increases, leading to improved control performance.

The use of DSP as a means of algorithm implementation requires the inclusion of two data converters, namely an analog to digital converter (ADC) and a digital to analog converter (DAC). The ADC samples the continuous time input signal, providing a discrete, digital input to the DSP. The DAC constructs a continuous, analog signal from the discrete outputs of the DSP. Both of these processes require low-pass filtering in order to preserve the information of the original signal and observe the desired output signal.

According to the Nyquist-Shannon sampling theorem, the sampling done by the ADC must be performed at a frequency at least twice as great as the highest frequency of significant content in the input signal.[20] This practice ensures that frequency content above twice the sampling frequency (or Nyquist frequency) is not aliased to frequencies below twice the sampling frequency. For practical applications, the ideal sample frequency seems to be between ten and twenty times the target frequency for control.[21] Filters known as anti-aliasing filters are inserted before the ADC to attenuate all frequencies above the desired control band. Appropriate anti-alias filters are crucial for

feedback control systems since aliasing would not only lead to unexpected noise in the error signal, but instability as well. On the other hand, minimal filtering is desired in order to shorten the overall system delay and maximize performance.

Additional filters, known as reconstruction filters, are placed at the output of the DAC. These filters have a smoothing effect on the quantization errors that result from discontinuities in the discrete time signal. Insufficient reconstruction filtering will lead to the creation of artificial high frequency content in the output signal. This becomes more of an issue of performance than stability since the anti-alias filters should keep any significant amounts of these higher frequencies from being fed back to the controller. Once again, minimal filtering will reduce system group delay and improve system performance.

3.6 Internal Model Control (IMC)

In order for the feedback control system depicted in Figure 3.1 of this thesis to work an ideal plant must be assumed. This does not take into consideration any delay from acoustical propagation or filtering. In other words, it would require the feedback path to be perfectly accurate and instantaneous. The concept of group delay was introduced in an earlier chapter as part of a discussion on the ability to control fan noise. The delays and signal alterations introduced by acoustical propagation, transducers, filters, and other electronic hardware need to be taken into consideration as a part of the plant when designing the controller, since they are significant contributors to the response of the closed loop system. One of the more successful methods of controlling a non-ideal plant requires the inclusion of an estimation of the plant response, known as an internal

model. The output of the control filter, *u(n)*, is filtered by the internal model of the plant and subtracted from the error signal, *e(n)*, to form an estimation of the original disturbance signal, *d(n)*. This becomes the new input of the control filter. This process, called the internal model control (IMC) method, is illustrated in Figure 3.3.

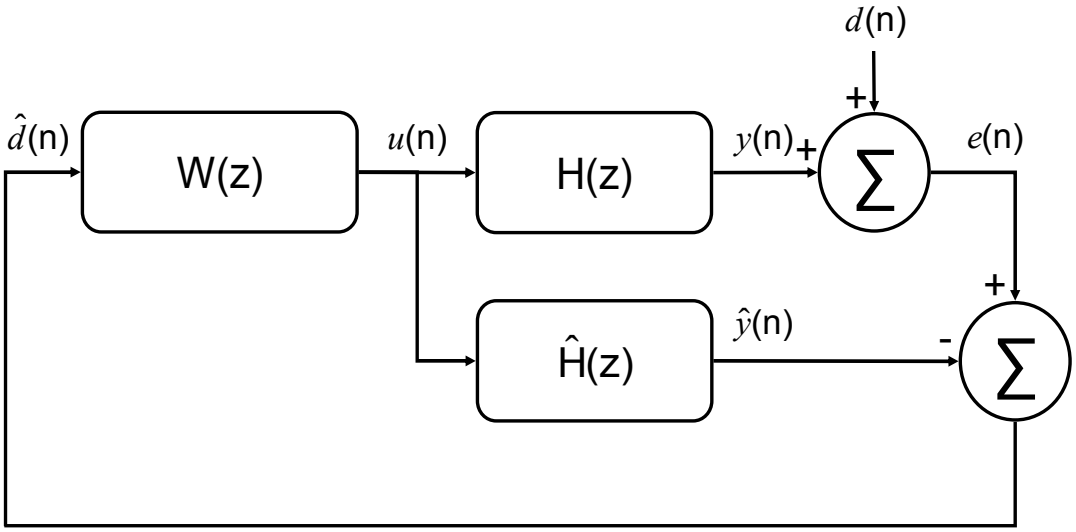

Figure 3.3 Block diagram of the IMC feedback control model.

3.7 Adaptive Control

Control becomes adaptive when one or more parameters of the controller are varied in real time as input and output data are observed by the system, effectively beginning with an approximation of the device to be controlled and converging to a more exact representation. This is desirable for maximizing the level of noise reduction achieved by the feedback control of axial fan noise. Adaptive control is also used to maintain stability and control performance in the event that the plant is altered. One of the benefits of digital controller implementation is the greatly increased ability to employ adaptive control. Quadratic minimization is an effective technique for ensuring the existence of a global minimum error signal and reaching it.

For the IMC control system, the error signal is a linear function of the control filter coefficients. Thus, a performance function, *J,* can be created to be a quadratic function of the control coefficients

$$J = E\{e^2(n)\}, \tag{3.3}$$

where E represents the expectation operator.

The greatest possible reduction of the error signal is achieved when the gradient of the performance function with respect to the control filter coefficients is zero, ie,

$$\frac{\partial J}{\partial W} = 0. \tag{3.4}$$

To obtain this optimal level of control in a stable and robust manor, the control filter coefficients are updated as

$$\bar{w}(n+1) = \bar{w}(n) - \mu e(n)\bar{r}(n). \tag{3.5}$$

where μ is the convergence parameter that determines the step size of the adaptations in the controller.

The complete adaptive control algorithm used for this research is illustrated in the block diagram of Figure 3.4. This form of the adaptive IMC algorithm was used by Kuo, *et. al.* and referred to as the adaptive feedback active noise control (AFANC) algorithm in their work on global attenuation of industrial machine noise.[12]

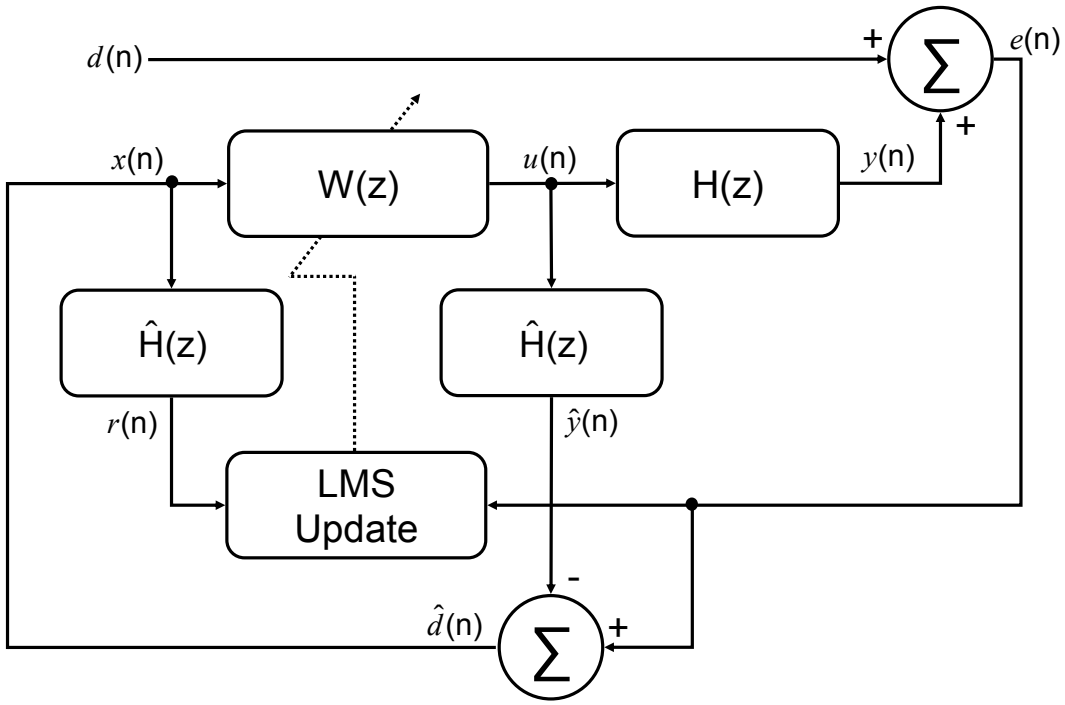

Figure 3.4 Block diagram of the adaptive feedback algorithm used for this research.

This algorithm makes use of a so called filtered-x signal similar to the FXLMS feed-forward algorithm from Figure 1.2. Since there is no reference signal coherent with the actual disturbance signal, *d(n)*, a reference is estimated from the error signal, *e(n)*. The actual disturbance signal is the difference between the error signal and the output, *y(n)*, which is estimated by filtering the output of the control filter, *u(n)*, with the estimation of the secondary path. The estimation of *d(n)* becomes the reference signal, *x(n)*.

3.8 Decentralized and Centralized Controllers

For a multi-channel control system, controllers may be designed in one of two fashions: decentralized or centralized. Decentralized control involves the development of multiple controllers, each independent of one another. This method is simple and

generally assumes negligible interaction between the different controllers. Centralized control involves the creation of a single controller, which is aware of each channel in the system and incorporates the interactions between them. Centralized control is often necessary for stability in systems with more than one control channel.

The success of the four-channel ANC system for small axial cooling fans is due largely to strong source coupling between the four control loudspeakers and the fan at low frequencies. However, the control sources themselves are also close to each other when compared to the wavelength of their output signals. The distance between any two adjacent control speakers is 80 mm, making the diagonal distance approximately 113 mm. The real part of the mutual impedance, Re(Z_{ab}), between any two identical sources is calculated as a function of frequency and distance:

$$\mathrm{Re}\left[Z_{ab}\right] = \mathrm{Re}\left[Z_{aa}\right] \times \frac{\sin(kd)}{kd}. \qquad (3.6)$$

This is the same relationship as Equation 1.5.

Figures 3.5 and 3.6 contain plots of the mutual impedance strengths relative to the self-impedance for equal sources versus frequency for a distance of 80 mm and 113 mm, respectively.

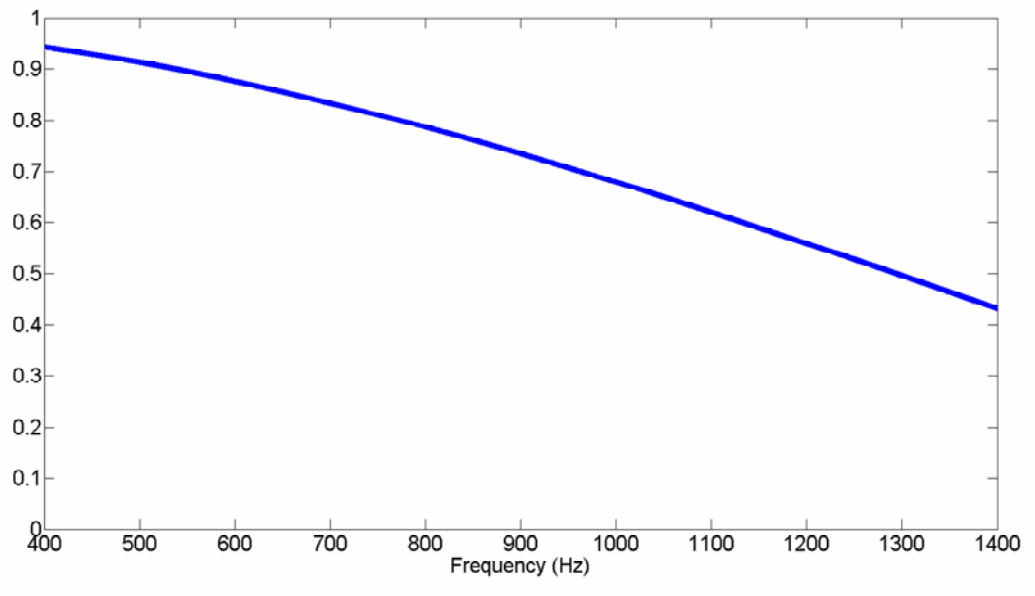

Figure 3.5 Normalized mutual impedance for two identical sources at a distance of 80 mm.

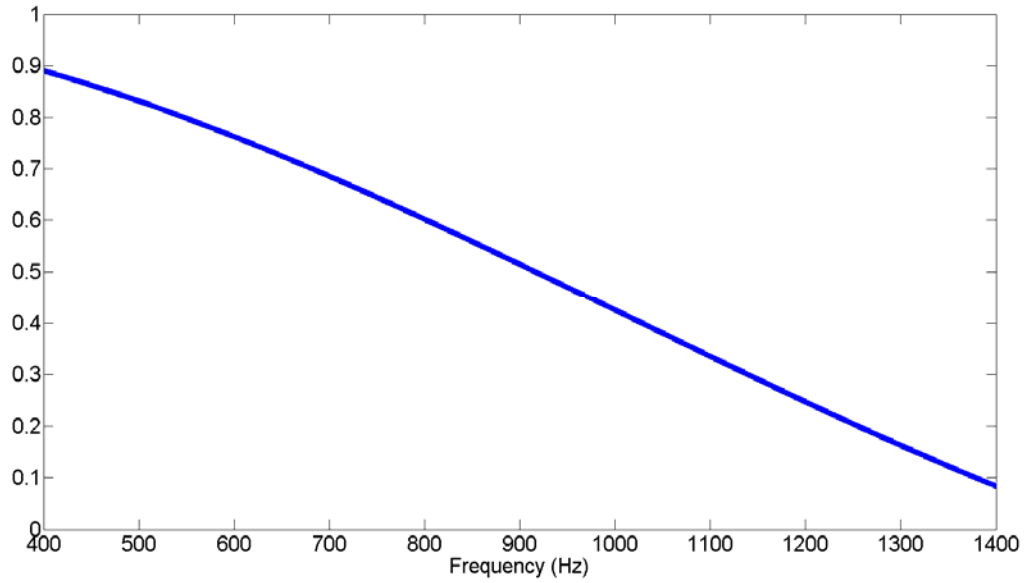

Figure 3.6 Normalized mutual impedance for two identical sources at a distance of 113 mm.

Mutual impedances due to the other three sources constitute a substantial part of the total radiation impedance for each of the control loudspeakers. This suggests that a

centralized controller would be desired for optimal performance, if not necessary for stability in the four-channel ANC system. One of the goals of this research was to observe and compare the performance of both systems and to make a recommendation as to which is more desirable for this specific application. These results are presented in Chapter 6.

3.9 Feed-forward/Feedback Hybrid Control

It is generally accepted that an adaptive feed-forward ANC system will outperform a feedback ANC system as a means of attenuating a periodic signal. This is a result of the incredibly high coherence usually achieved between the reference and error signals of the feed-forward system when compared to the level of autocorrelation in the error signal after a realistic group delay. However, feedback ANC has already been established as a logical solution for control of a noise source that lacks a properly coherent reference signal. A controller with both feed-forward and feedback components might successfully reduce tonal noise related to the BPF as well as broadband noise and tonal content unrelated to the BPF.

In order to investigate the likely results of such a hybrid noise control system, the two systems were joined as a part of the research for this thesis. The FXLMS algorithm (Figure 1.2) was implemented on one set of DSP hardware while the adaptive IMC algorithm (Figure 3.4) was implemented on another set of DSP hardware.

CHAPTER 4

EXPERIMENTAL SETUP

4.1 Mock Computer Case

The fan was installed in a mock computer case constructed of aluminum panels mounted on an aluminum frame. The interior has been damped with carpet and foam to dampen the resonances of the enclosure. The computer case is 16.5 inches tall, 8.5 inches wide and 18.5 inches deep. A hole, roughly 1 inch by 2 inches, was cut into the front panel of the box to accommodate the flow of air and the insertion of cables. Figure 4.1 contains a photograph of the mock computer case.

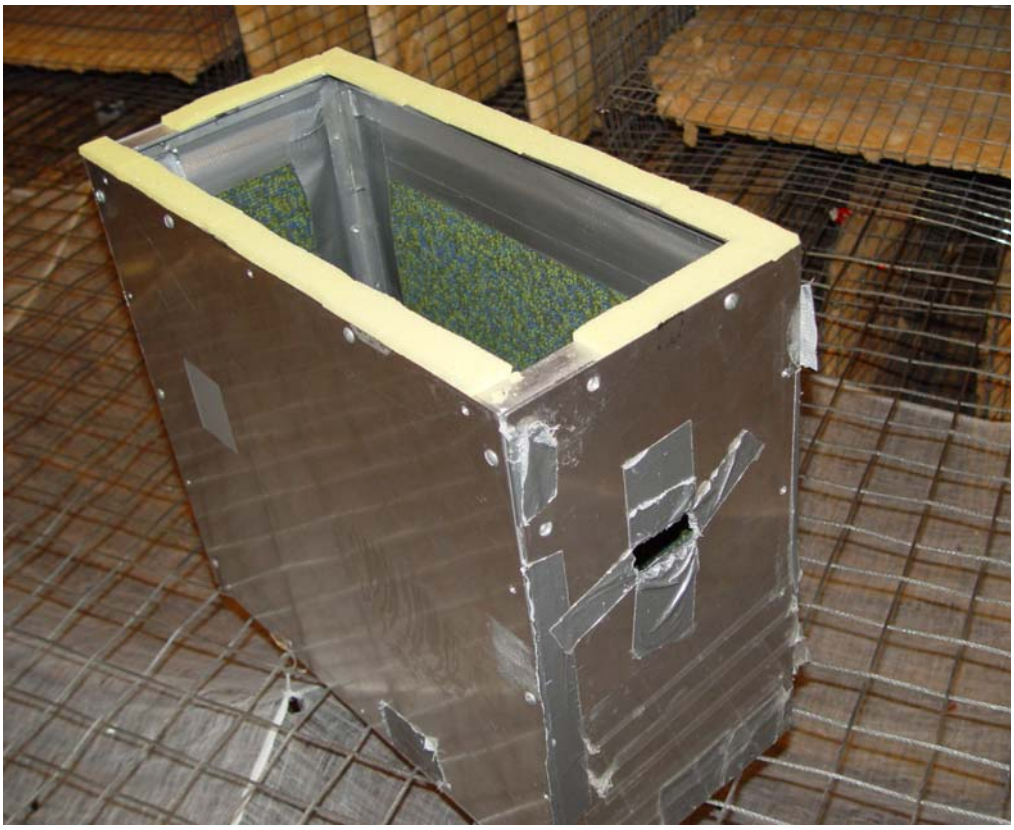

Figure 4.1 Mock computer case used to house fans for ANC research.

4.2 Fan

The fan used for experimental procedures was a 60mm Mechatronics® 12 volt DC brushless axial cooling fan, which is typical of the type of fan that would be used for cooling in a desktop computer. This was the same fan used in the results published by Monson and Sommerfeldt for control of tonal noise radiating from an axial cooling fan.[22]

Each different algorithm and system configuration was tested with a 2 inch loudspeaker acting as the primary source before the fan was installed. This was done so that the noise of the primary source could be band limited and its source strength could be chosen, which reduced the number of variables in comparing performance from one setup to another. It was also helpful to test feedback control on broadband noise that was not caused by flow, as a benchmark for later tests.

4.3 Control Sources

Four equally spaced loudspeakers were used as secondary sources for control. This source configuration provides for optimal control of the primary source and is symmetrical for ease of implementation. The loudspeakers are 1 inch, high excursion, wide-range drivers. They are bulkier than the speakers that were used for tonal control of the same fan, but offer a flatter frequency response which extends to lower frequencies. They are also capable of much higher output levels. A photograph of one of the control loudspeaker drivers is found in Figure 4.2

Figure 4.2 1" Loudspeaker used as secondary source for ANC.

The control loudspeakers were mounted with an adhesive to the aluminum plate where the fan resided. Small enclosures were constructed from PVC pipe caps and attached to the back of the plate as shown in Figure 4.3, in an attempt to improve the performance of the loudspeakers. The enclosures were not optimized for performance or to conserve space in the mock computer case. They were simply a way to conveniently provide an enclosure so that the driver could radiate more efficiently.

Figure 4.3 PVC pipe cap loudspeaker enclosures used for secondary sources.

4.4 Error Sensors

Small electret microphones were used as error sensors. The electret microphones require a five volt bias for power and considerable amplification to ensure a clean, accurate representation of the noise they are actually exposed to. A small preamplifier was constructed to provide the needed bias voltage and a gain of approximately 200 to the output signals of the microphones. Also included was a single-pole, high-pass RC filter with a cutoff frequency of 800 Hz in order to attenuate some low frequency noise presumably caused by the flow of the fan. The microphones were positioned in near-field positions in the same plane with the fan and control speakers. A set of ideal in-

plane positions for microphone placement was determined by the method developed by Gee and Sommerfeldt.[7] Calculated ideal locations are frequency dependant. However, there exist certain positions of maximum pressure attenuation that do not vary much with frequency. Actual error sensor positions were selected from the set of ideal positions that varied least with frequency. The decision for the final microphone locations was based on desired proximity to the primary and secondary sources. Placing the microphones too close to the fan would expose them to high amounts of turbulent flow, thus leading to an unfavorable signal to noise ratio (SNR) for the error signal. Also, it is desirable to place the error microphones as close as possible to the secondary sources as a method of minimizing group delay. Figure 4.4 includes the cooling fan, control loudspeakers, and error sensors all mounted in an aluminum plate on the mock computer case.

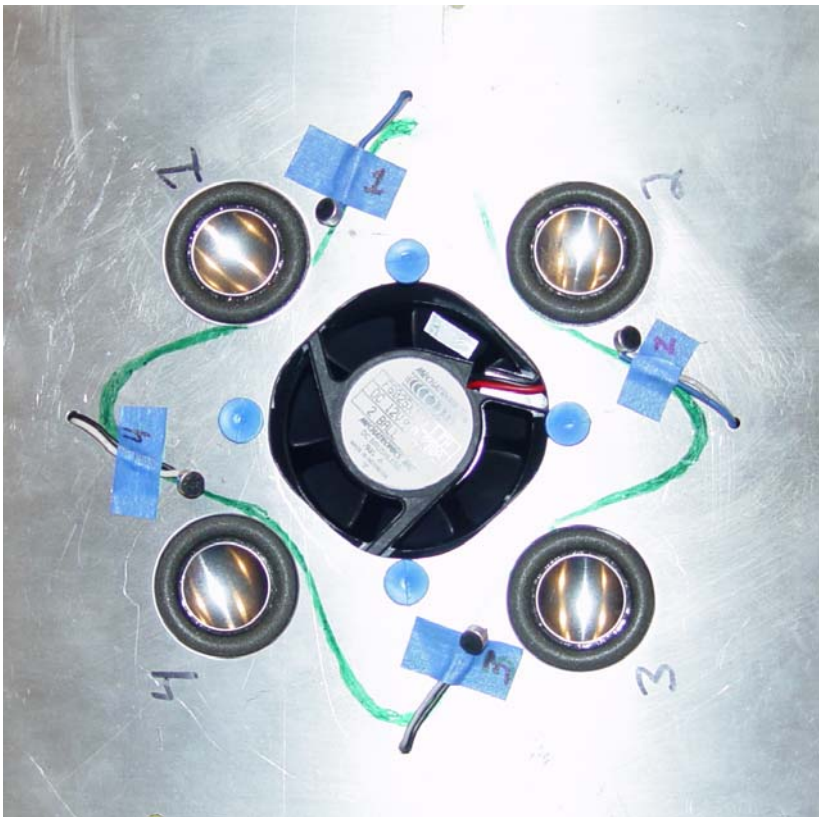

Figure 4.4 Cooling fan, control loudspeakers, and error microphones mounted in the top plate of the mock computer case.

Figure 4.5 shows this same ANC hardware arrangement with the 60 mm cooling fan being replaced by the two-inch loudspeaker as discussed in Section 4.2.

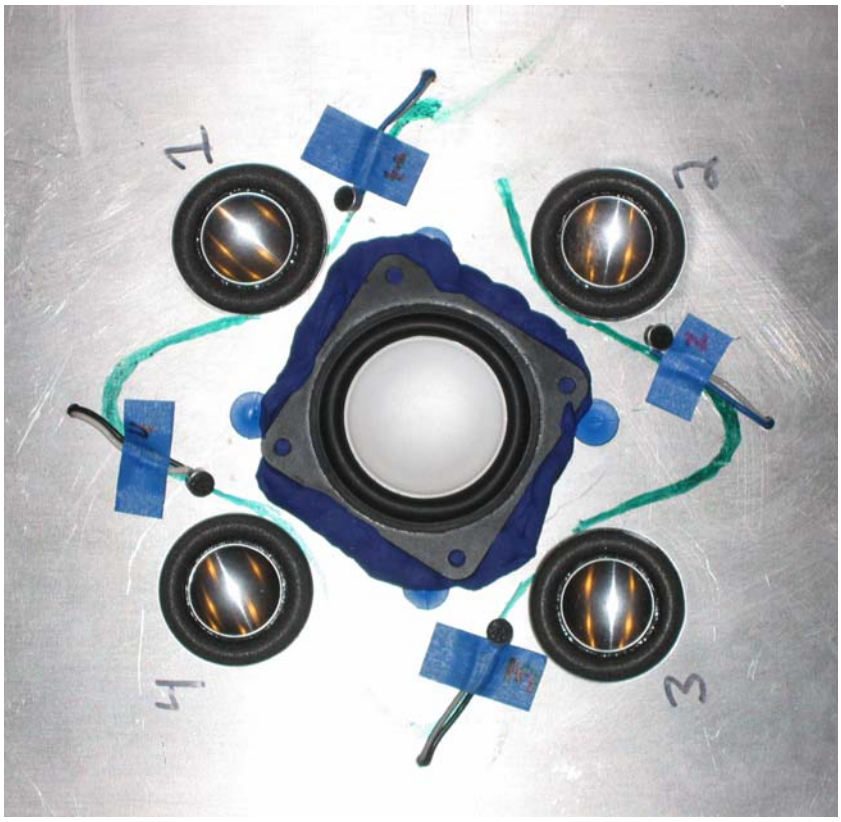

Figure 4.5 Primary source loudspeaker, control loudspeakers, and error microphones mounted in the top plate of the mock computer case.

4.5 DSP and Electronics

Control algorithms for this research were run on a Texas Instruments TMS320C6713 digital signal processor, capable of performing 1350 million floating point operations per second (MFLOPS). The DSP chip was bundled with a power supply, memory, and an input/output (I/O) interface card by Traquair Data Systems, Inc.

The DSP board and enclosure are pictured in Figure 4.6. For this research, a sample frequency of 6 kHz was chosen.

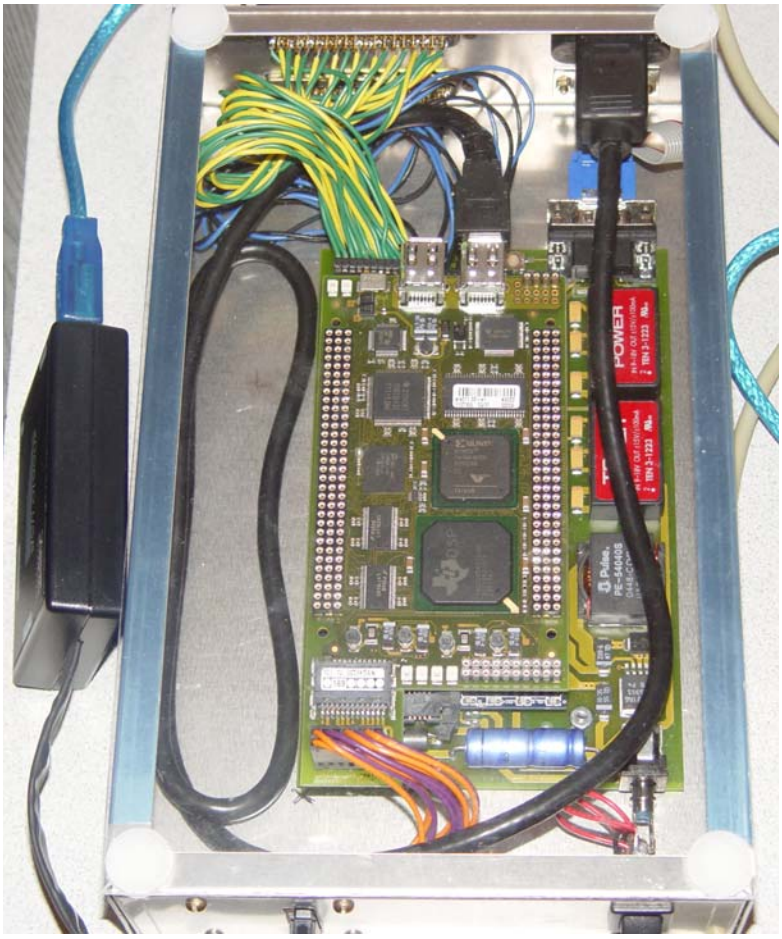

Figure 4.6 DSP system purchased from Traquair, bundled in an enclosure designed by Benjamin Faber at Brigham Young University.

A module containing variable filters and gain stages was designed to condition the analog input and output signals. The module is configured for up to eight analog input channels and up to four analog output channels. Each of the input channels has a fifth order switched capacitor Butterworth filter for use as an anti-alias filter, along with fine and coarse gain adjustments. Each channel of output has a switched capacitor filter, identical to the input filters, for use as a reconstruction filter. The levels of the output

channels are also adjusted by fine and coarse adjust gain stages. A photograph of this completed module is found in Figure 4.7

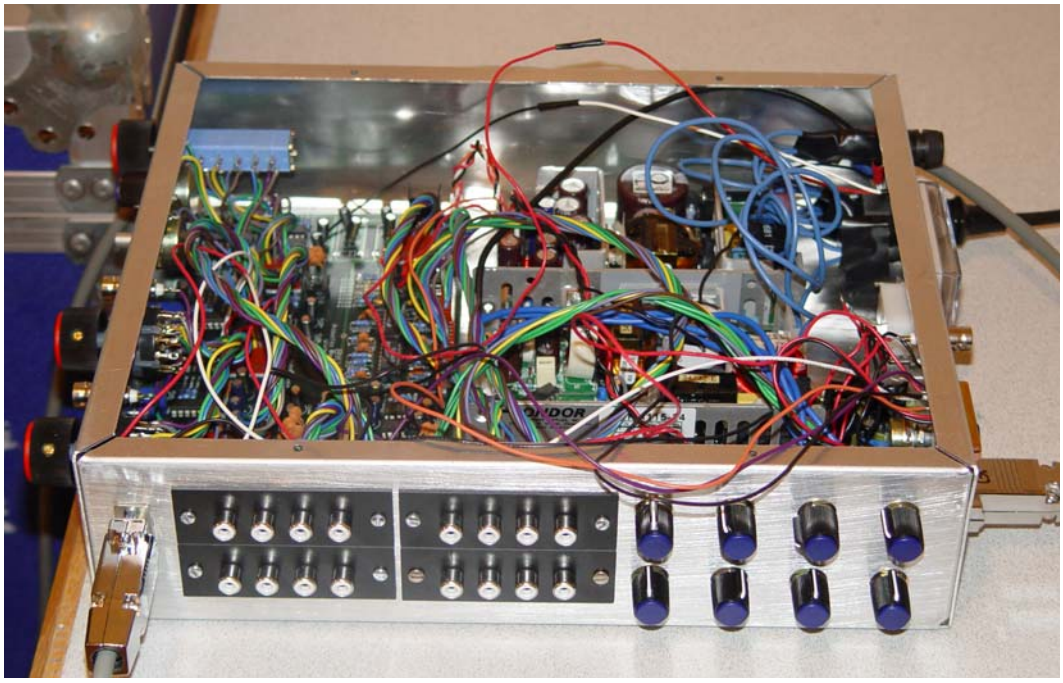

Figure 4.7 Analog signal conditioning hardware designed by Benjamin Faber and Brian Monson at Brigham Young University.

Two ten watt stereo power amplifier kits were assembled in a separate module to provide the current gain needed for driving the load of the control loudspeakers. The actual power output of the secondary sources while running control was observed to be approximately ten milliwatts. However, most of the hardware used in this research was designed as flexible equipment that could be used in many different but related projects.

In order to band-limit the error signals for stability and decrease overall system group delay for performance, the reconstruction filters in the above mentioned signal conditioning hardware were removed and replaced by single-pole, low-pass RC filters in the power amplifier module with cutoff frequencies set at 1.2 kHz. The switched

capacitor filters that remained as anti-alias filters were set with a cutoff frequency of 2.7 kHz.

4.6 Measurements

Measurements for this research were taken in an anechoic chamber at Brigham Young University, as seen in Figure 4.8. The chamber is fully anechoic down to 75 Hz and measurements taken therein were done using a semicircular boom, also shown in Figure 4.8. The boom holds 13 half-inch ICP microphones spaced at fifteen-degree intervals and the boom is rotated azimuthally in fifteen-degree intervals for global measurements.

Figure 4.8 Photograph of BYU anechoic chamber and semi-circular microphone boom used for global measurements of fan noise reduction.

CHAPTER 5

MEASUREMENTS AND RESULTS

5.1 Analog Feedback Control

Using a loudspeaker as the primary source, the single-channel analog controller was used to control band-limited white noise provided by a function generator. The reduction achieved is presented as a function of frequency in Figure 5.1. There are two functions on this plot, one for an error microphone placed in an ideal location for global control according to Gee and Sommerfeldt and one in an arbitrarily chosen location not included as one of the suggested positions for ideal global control.

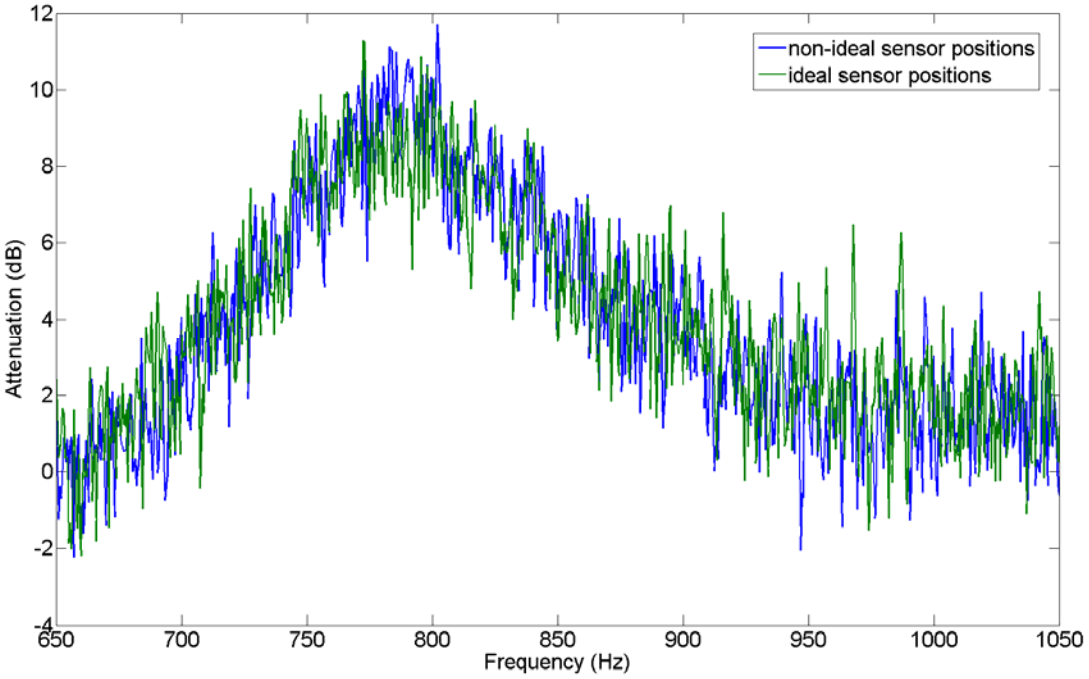

Figure 5.1 Reduction of band-limited white noise levels (in dB) achieved by a single-channel analog controller at the error sensor.

The region where control operated effectively was very narrow, mostly between 700 Hz and 900 Hz. This was due largely to the frequency response of the control source. The loudspeaker used for control in this experiment was a smaller driver with a

nonuniform frequency response. Its response had a considerable resonance at about 800 Hz and rolled off quickly for lower frequencies. Considering that the product of the acoustical wavenumber and the distance between primary and secondary sources, or *kd* value, for the physical system was approximately 0.7 at 800 Hz, the analog controller performed well across this narrow band, according to the theory of Nelson and Elliot shown in Figure 1.3. Also, the position of the error microphone seems to have no measurable effect on the ability of the controller to attenuate the signal at the error sensor. Figure 5.2 contains a plot of the far-field levels of attenuation for the same system.

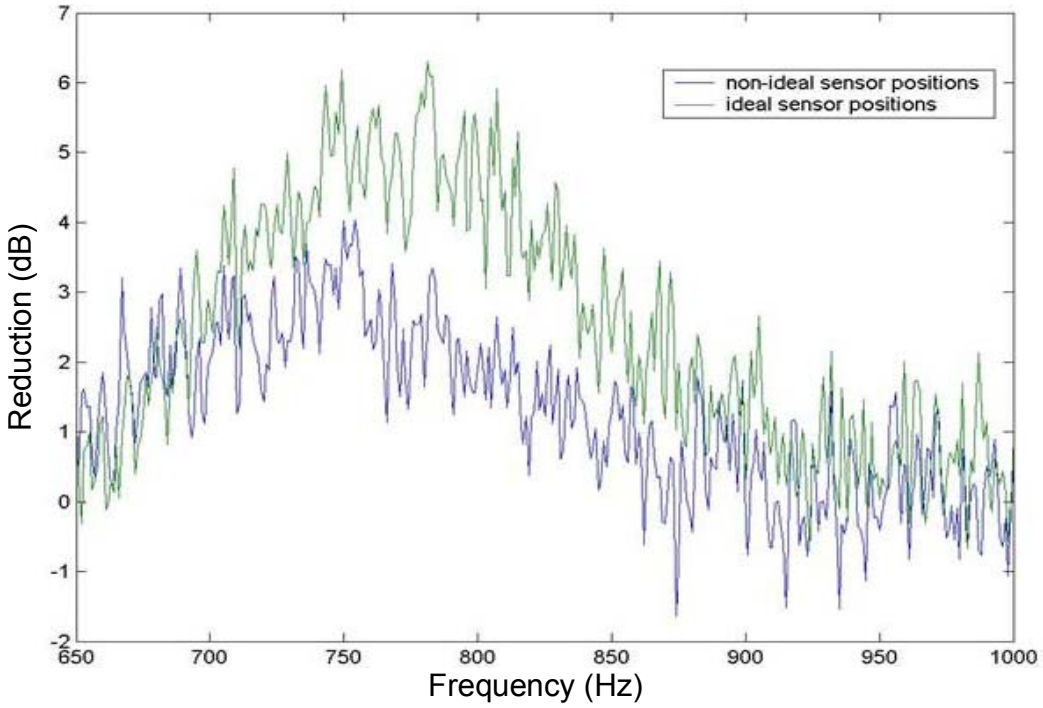

Figure 5.2 Reduction of band-limited white noise levels (in dB) achieved by a single-channel analog controller in the far field.

The attenuation seen in Figure 5.2 was global in nature and the difference can be observed between the controller with an ideally placed error sensor and one with a non-ideally placed error sensor.

The loudspeaker primary source was replaced with the 60 mm axial cooling fan. The global, far-field levels of attenuation are plotted in Figure 5.3.

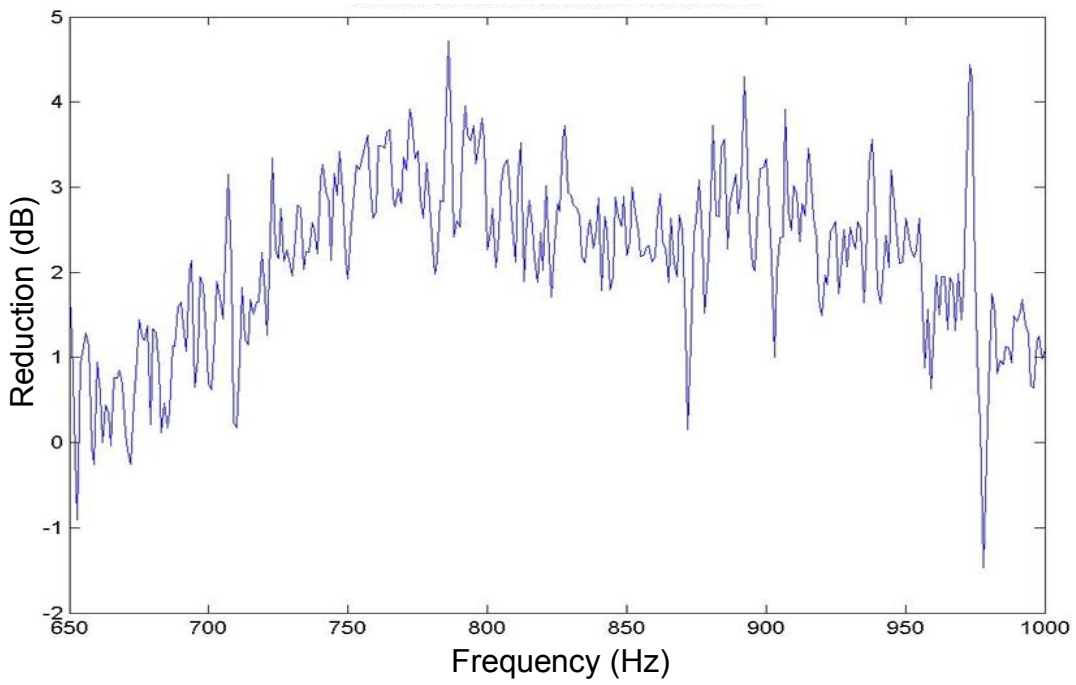

Figure 5.3 Reduction of axial cooling fan noise levels (in dB) achieved by a single-channel analog controller globally in the far field.

Since the majority of broadband fan noise content is caused by flow and is less deterministic than the band-limited signal sent to the loudspeaker primary source, it is expected that the levels of attenuation would be lower for the fan primary source. However, significant global reduction was still achieved. The measurements from the microphone boom were used to create a spatial representation of the noise reduction, as seen in Figure 5.4. This particular plot shows the fan noise reduction at a single frequency of 900 Hz. The outer mesh is characteristic of the noise source by itself and the solid inner mass is representative of the noise source with ANC. For the outer mesh, the radius is proportional to the sound pressure level in each direction. For the inner

color mass, both the radius and the color are proportional to the sound pressure level after ANC has been applied. These spatial plots provide visual verification of the global nature of the noise reduction.

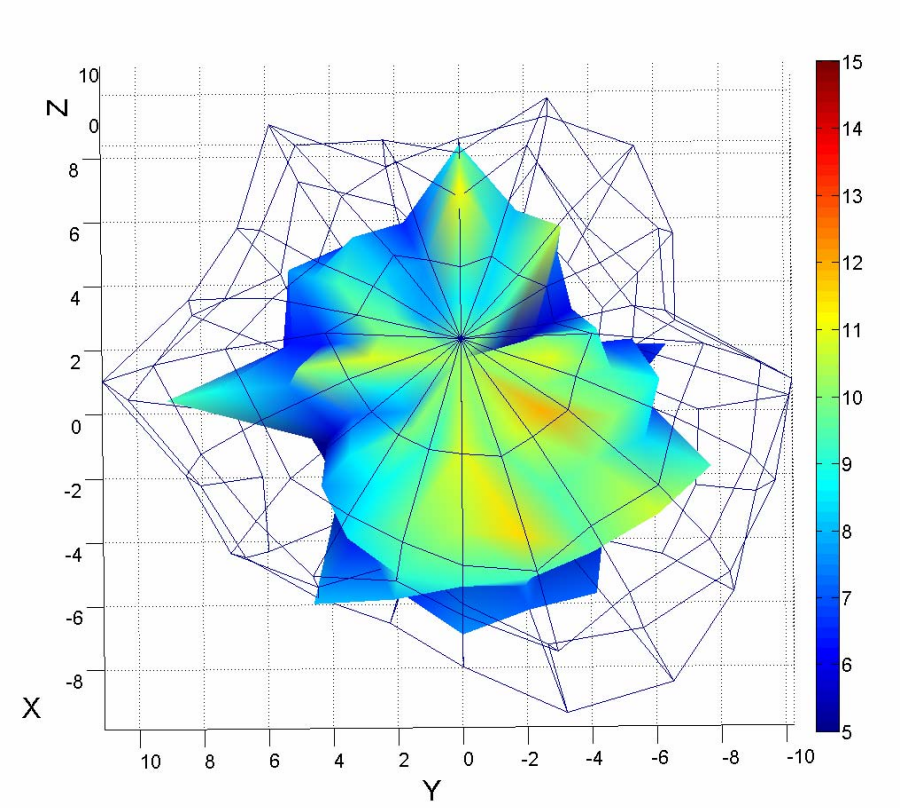

Figure 5.4 Spatial representation of the reduction of axial cooling fan noise (in dB) at 775 Hz achieved by a single-channel analog controller globally in the far field.

5.2 Autocorrelation Based Control Predictions

The results of several measurements were used to verify the accuracy of control predictions taken from autocorrelation measurements, as demonstrated in Section 2.4 of this thesis. These and all other measurements discussed in the remainder of this chapter involve digital controllers. Comparisons were made between the autocorrelation based predictions and the actual global reduction for loudspeaker and fan primary sources. The autocorrelation measurements used for control predictions were calculated from the error

sensor signals. This means that predicted reductions are for the entire frequency range where the system is capable of responding. It is not correct to limit the frequency bandwidth of the error signals in order to obtain an estimation of possible reduction over that certain bandwidth, because by limiting the bandwidth of a signal one artificially increases the amount of correlation in the signal. More meaningful evaluations of system performance will be presented later when the noise attenuation of specific frequency bands is observed.

A plot of the autocorrelation function for the band-limited white noise played through the loudspeaker control source is found in Figure 5.5, as measured by one of the error sensors.

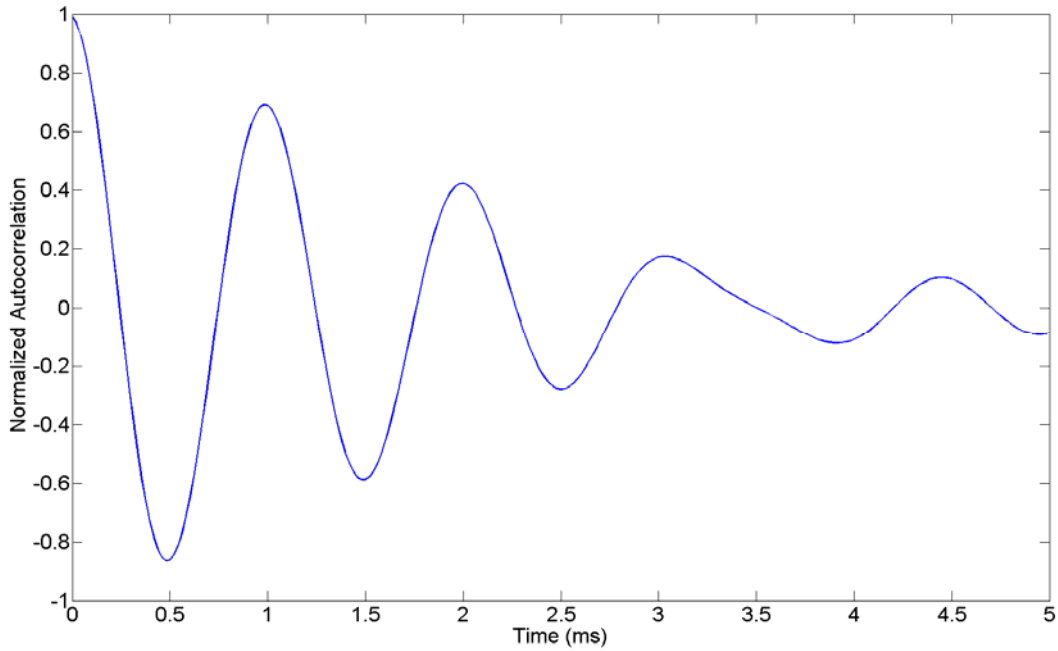

Figure 5.5 Normalized autocorrelation function for band-limited white noise played through the loudspeaker, measured by an error microphone.

The ANC system controller for the loudspeaker primary source was a decentralized adaptive filter with 200 coefficients. The system had a measured group

delay of 1 ms. Figure 5.5 shows that the maximum level of correlation after 1 ms. is 0.674. Equation 2.3 was used to predict the amount of attainable prediction for this noise source, where $E_p = 0.674$ and $E_{total} = 1$. This is demonstrated as

$$-10 \times \log\left(1 - \frac{0.674}{1}\right) = 4.9\ dB. \tag{5.1}$$

According to the prediction model an overall reduction of 4.9 dB could be expected.

The reduction obtained by the controller is plotted in Figure 5.6. The measured far-field noise attenuation was 4.1 dB. All of the global, far field power spectra, $P(f)$, in this thesis were calculated as

$$P(f) = 10 \times \log\left(\frac{\sum_{n=0}^{N-1} \frac{p_n(f)^2}{ref^2}}{N}\right), \tag{5.2}$$

where N is the number of microphone positions used for the global measurement, $p_n(f)$ is the pressure level measured at microphone position n, and ref is 20 µPa.

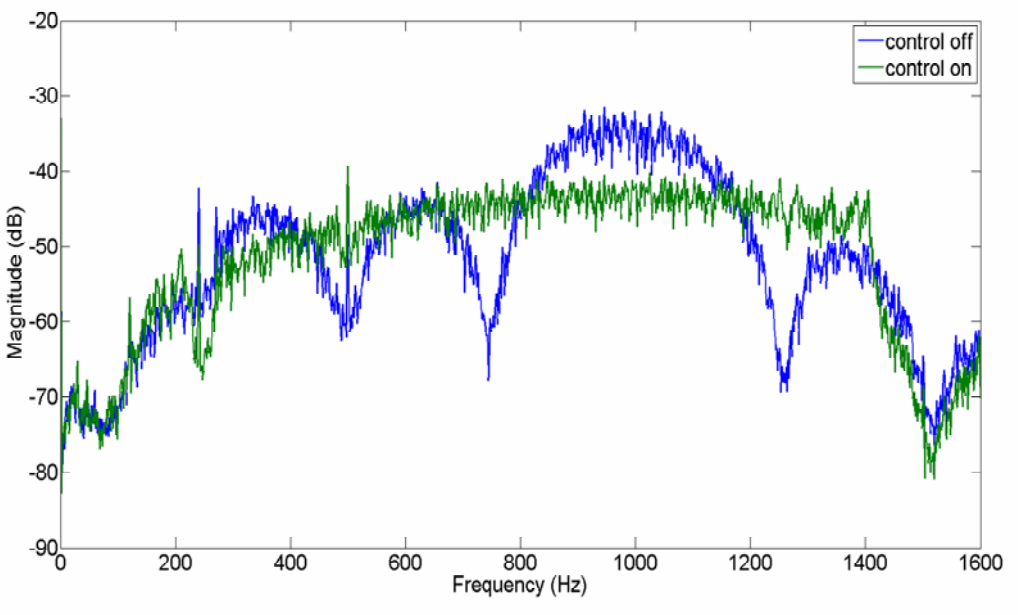

Figure 5.6 Auto power spectra of band-limited white noise levels played through the primary source loudspeaker and measured in the far field, with and without ANC.

The same control system was also used for the 60 mm axial cooling fan primary source. The autocorrelation function for the fan has been previously shown in Figure 2.1. Based on the control prediction model, an overall noise reduction of 0.5 dB is expected. Figure 5.7 contains a plot of the measured global noise reduction for the fan. The measured noise attenuation was 0.5 dB.

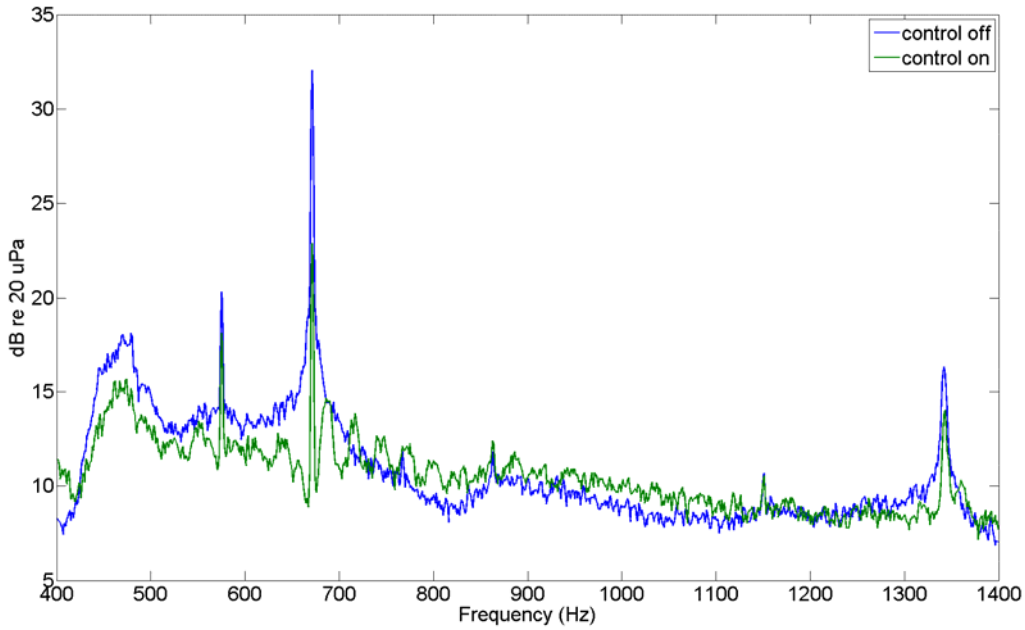

Figure 5.7 Auto power spectra of 60 mm fan noise (in dB) measured globally in the far field, with and without ANC.

5.3 Adaptive Control

Measurements were made in order to compare the performance results between an adaptive controller and a non-adaptive or static controller. The mock computer case was repositioned in the anechoic chamber so that it was approximately 15 cm away from a rigid wall on one side, as shown in Figure 5.8. The introduction of a rigid boundary provided a more complex and realistic secondary path.

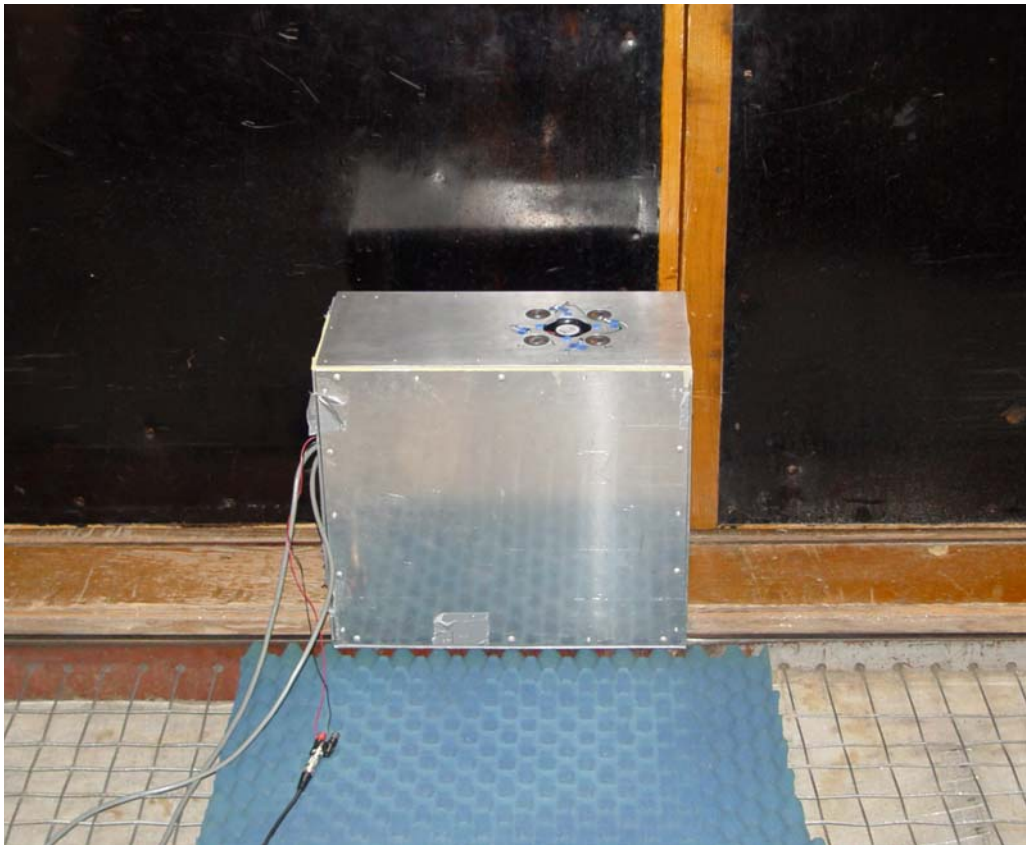

Figure 5.8 Mock computer case with fan and ANC system relocated to rigid wall within the anechoic chamber.

The static algorithm used in this study was a decentralized four-channel implementation of the IMC algorithm (see Figure 3.3). The adaptive algorithm was a decentralized four-channel implementation of the adaptive IMC algorithm, shown in Figure 3.4. Both the static and the adaptive control filters contained 200 coefficients per channel. The impulse response of the secondary path was measured for the new location of the fan and its coefficients were used as $\hat{H}$ for both the static and adaptive controller algorithms. The residual noise for each of the controllers is plotted along with the original noise levels in Figure 5.9. These results are taken from the signal produced by one of the error microphones and are therefore not calibrated, but are helpful as a means of comparison between the two algorithms.

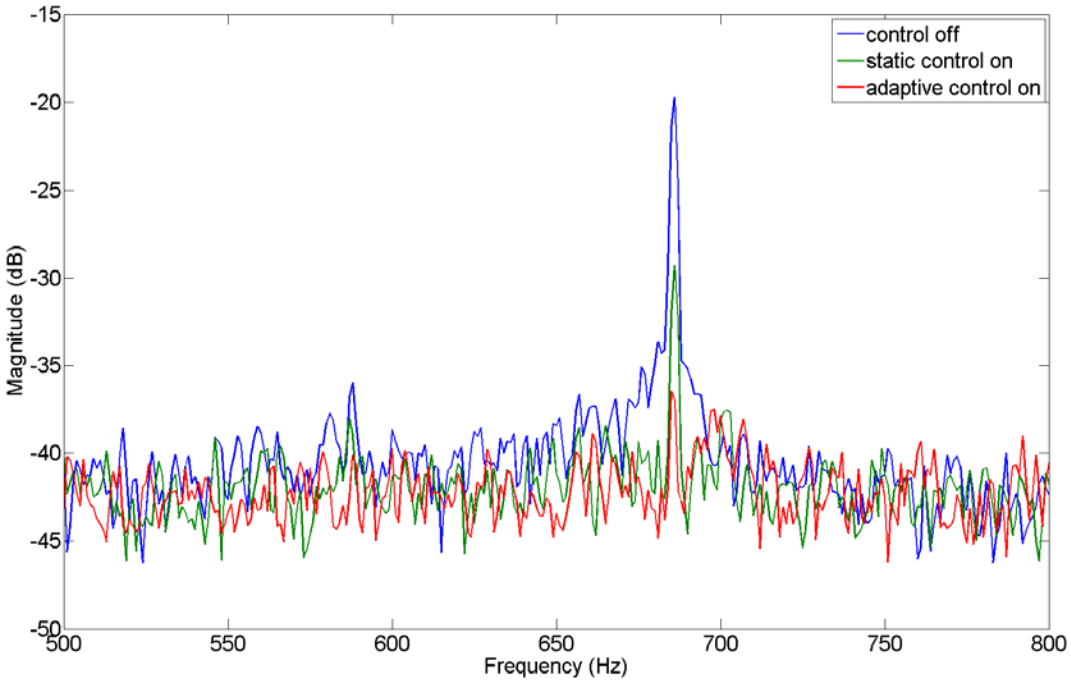

Figure 5.9 Auto power spectra (in dB) of fan noise, fan noise with static feedback ANC, and fan noise with adaptive feedback ANC.

The superior performance of the adaptive controller is seen by the graphical representation. The static controller reduced the overall levels between 500 Hz and 800 Hz by 3.6 dB at the error sensor. The adaptive controller reduced the overall levels within the same frequency range by 4.2 dB at the error sensor.

5.4 Decentralized and Centralized Control

The presence of source coupling between the four control sources surrounding the cooling fan was investigated and quantified in Section 3.8 of this thesis. It was important to understand the effects of secondary source coupling on the performance of the controller so that an educated decision could be made between decentralized and centralized control. The adaptive multi-channel IMC algorithm was used for a

comparison between a 64 tap decentralized controller and a 64 tap centralized controller. Noise attenuation was evaluated for both of the systems in the frequency range between 400 Hz and 1.4 kHz. Performance, when measured at the error sensors, was almost identical for the two different controller types. Figure 5.10 shows the residual noise at one of the error sensors for the decentralized and centralized controllers, compared to the fan noise without control. Both controllers attenuated the noise at the error signal by 1.6 dB over the target frequency range.

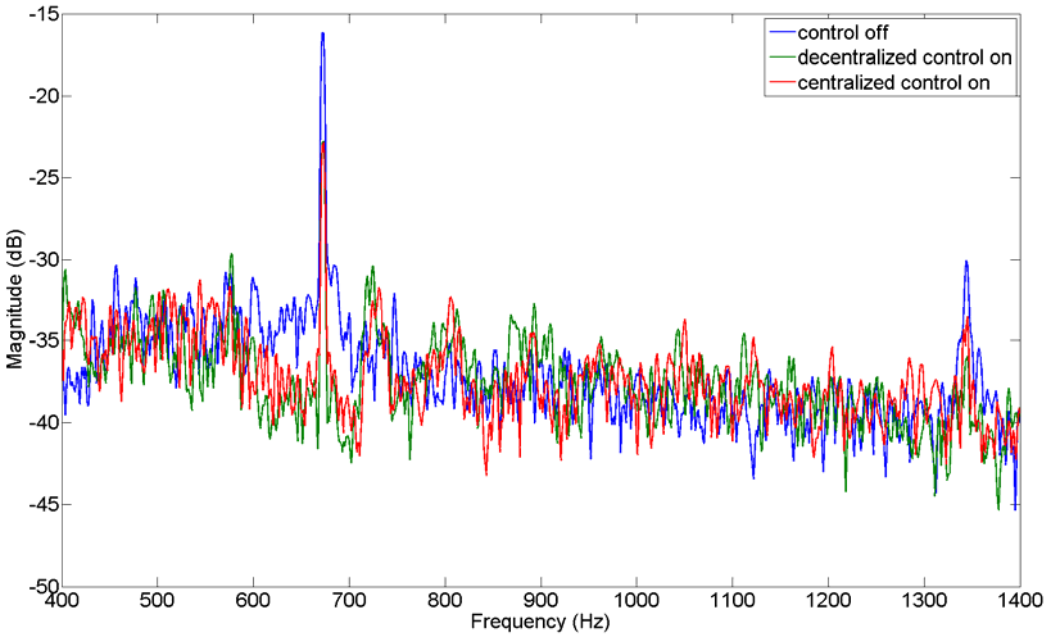

Figure 5.10 Auto power spectra of fan noise with and without centralized and decentralized adaptive feedback ANC as measured (in dB) at an error sensor.

The results achieved by the two controllers differed more in the far-field. The decentralized controller produced a global reduction of 0.8 dB over the target frequency range, while the centralized controller produced a global reduction of 0.5 dB over the same frequency range. Figures 5.11 and 5.12 provide plots of the reduction achieved by each system.

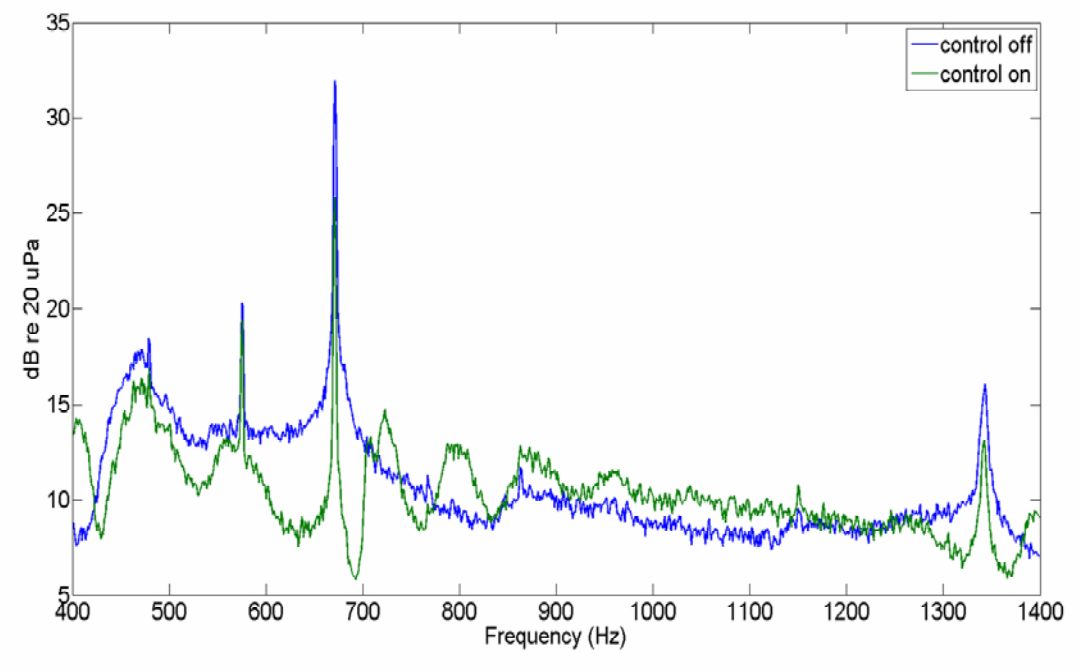

Figure 5.11 Auto power spectra of fan noise with and without decentralized adaptive feedback ANC.

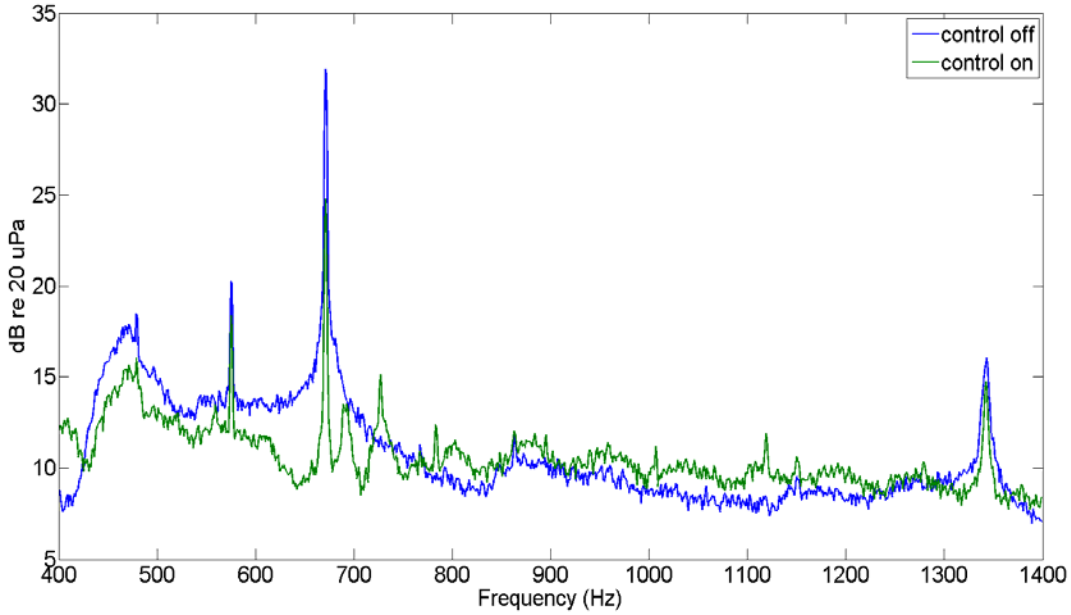

Figure 5.12 Auto power spectra of fan noise with and without centralized adaptive feedback ANC.

The residual power spectrum of the noise controlled by the centralized controller is slightly more uniform than that of the one controlled by the decentralized controller. However, the decentralized controller is more aggressive near the BPF and second harmonic.

The source coupling between the secondary sources is not adversely affecting stability when it is ignored in the controller. This is likely due to the fact that all four control sources are in phase with each other. This ensures that source coupling can only serve to increase the radiated power from each source, and is incapable of causing cancellations between two or more of the sources. An increase of radiated power from a secondary source would only be a problem if the controller was not adaptive. The updating of the control filter compensates for any unexpected boosts in radiation efficiency at the secondary sources. This explains why, in this particular situation, the control algorithm is capable of minimizing the correlated portion of the noise signal at the error sensor whether the controller is centralized or decentralized.

However, centralized control gains an advantage over decentralized control in global measurements. This is likely due to the fact that the model described in Section 1.3 of this thesis for calculating proper locations for error microphones in the near field does take into account the coupling between the control sources. Since the decentralized controller is unaware of how much each control loudspeaker is contributing to the reduction at each microphone, the pressure in the near field might look differently than expected in places other than the four microphone locations. This would lead to variations from the expected minimization in the far-field pressure.

The centralized and decentralized controllers each produced flatter residual responses and greater levels of overall attenuation as the number of filter coefficients was increased. The centralized controller became too computationally expensive for the DSP at about 70 filter coefficients. The DSP was capable of running over 200 coefficients with a decentralized controller. The best performance was obtained from a decentralized controller with 200 coefficients. Results from this controller are presented in Section 5.6 of this thesis.

If centralized control would have demonstrated significant benefits over decentralized control, a third system would have been designed and tested with the goal of taking some secondary source coupling effects into consideration while maintaining more of the simplicity of a decentralized controller.

5.5 Feed-forward/Feedback Hybrid Control

The FXLMS feed-forward algorithm was implemented using 64 control taps on the same hardware used for the feedback research. The narrowband attenuation (focused on the BPF) provided by the feed-forward control attenuated the total noise in the 400 Hz to 800 Hz frequency band by 0.5 dB. This reduction is illustrated in Figure 5.13. Figure 5.14 provides a view of the combined efforts of narrowband feed-forward control and broadband feedback control, which provided 1.0 dB of global attenuation.

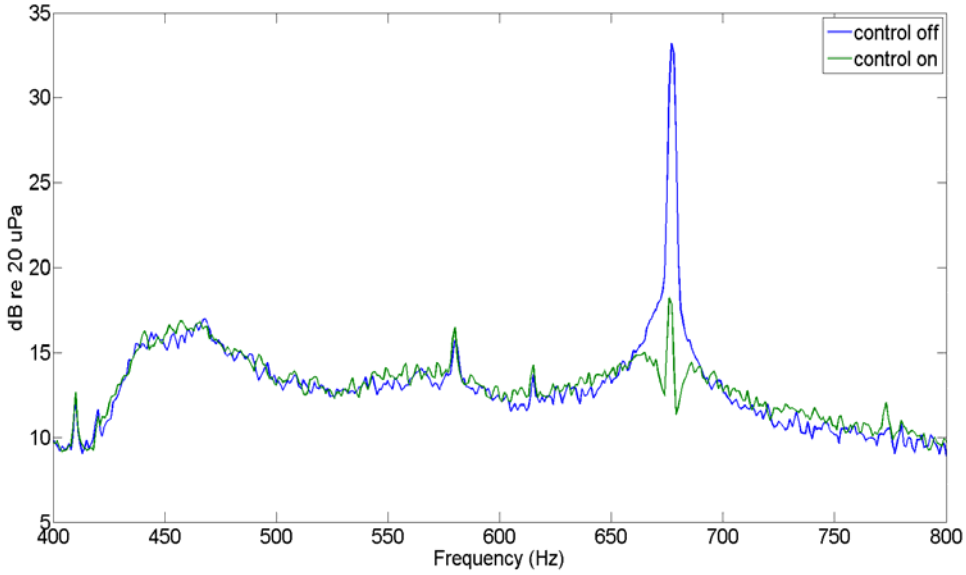

Figure 5.13 Global feed-forward control of narrowband tonal fan noise.

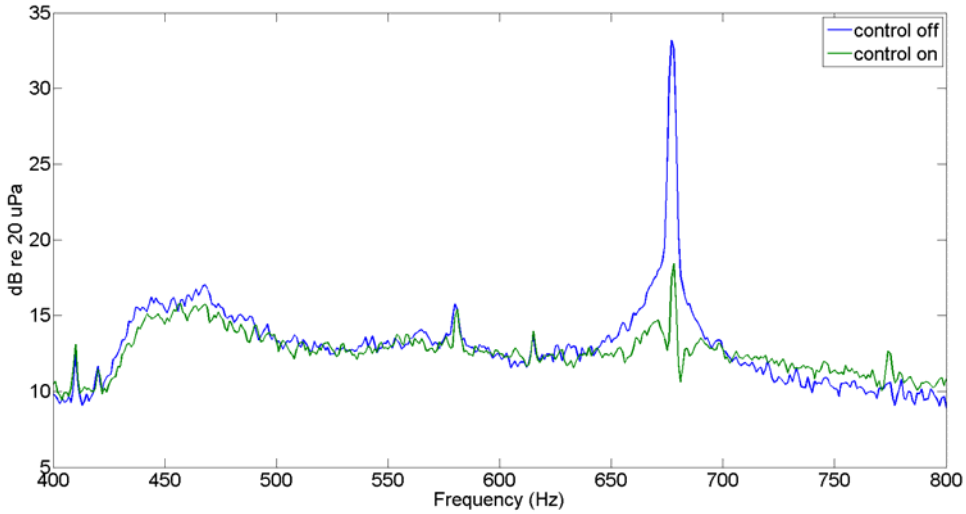

Figure 5.14 Global feed-forward control of narrowband tonal fan noise combined with feedback control of broadband fan noise.

The strengths of the two systems appear to combine without inhibiting each other. The feed-forward control performed well on the noise at the BPF and the feedback

control decreased some of the low frequency broadband noise unseen by the feed-forward controller.

5.6 Final Results

The most effective feedback system included a four-channel, decentralized adaptive IMC controller with 200 control coefficients per channel. This system provided 0.9 dB of global nose reduction in the frequency range between 400 Hz and 1.4 kHz, as is shown in Figure 5.15.

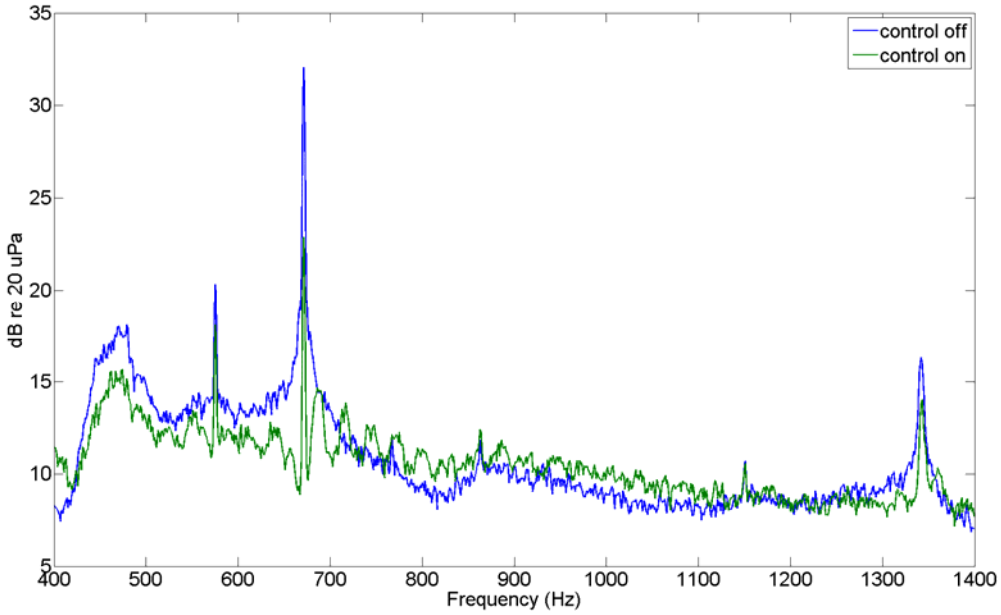

Figure 5.15 Four-channel, decentralized, global adaptive feedback control of broadband fan noise with 200 control taps.

Figure 5.16 is a spatial representation of the same measurements used to generate Figure 5.15. Since the overall attenuation is small there is not a large gap between the outer mesh and inner mass. However, since the outer mesh is visible in all places the controlled noise is always at a lower level than the uncontrolled noise. This type of plot

was used earlier, in Figure 5.4, to show global reduction at a single frequency. The calculation required for broadband spatial representations of noise reduction is as follows,

$$r(n,\theta) = 10 \times \log\left(\sum_{f=a}^{b} \frac{p^2(n,\theta,f)}{ref^2}\right). \qquad (5.3)$$

The outcome, $r(n,\Theta)$, is the sound pressure level at microphone n on the boom that has been rotated Θ degrees. The input, $p^2(n,\Theta,f)$, is the squared pressure magnitude measured from that same microphone at a rotation of Θ degrees, for a frequency, f. The letters a and b are the lower and upper frequencies of interest, respectively, for the broadband evaluation. The variable, *ref*, is 20 µPa.

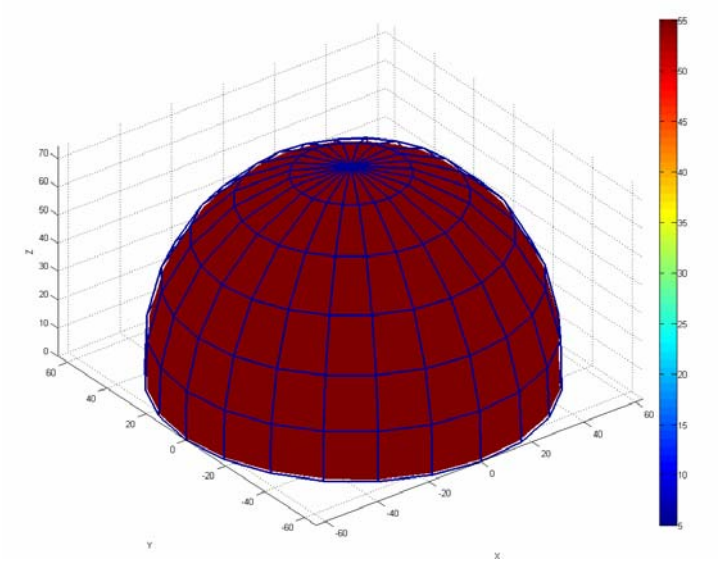

Figure 5.16 Spatial representation of multi-channel, decentralized, adaptive feedback control of broadband fan noise with 200 control taps.

Figure 5.17 contains a spatial plot of the narrowband attenuation, similar to Figure 5.16, but focused near the BPF. The BPF tone was reduced globally by 10.4 dB.

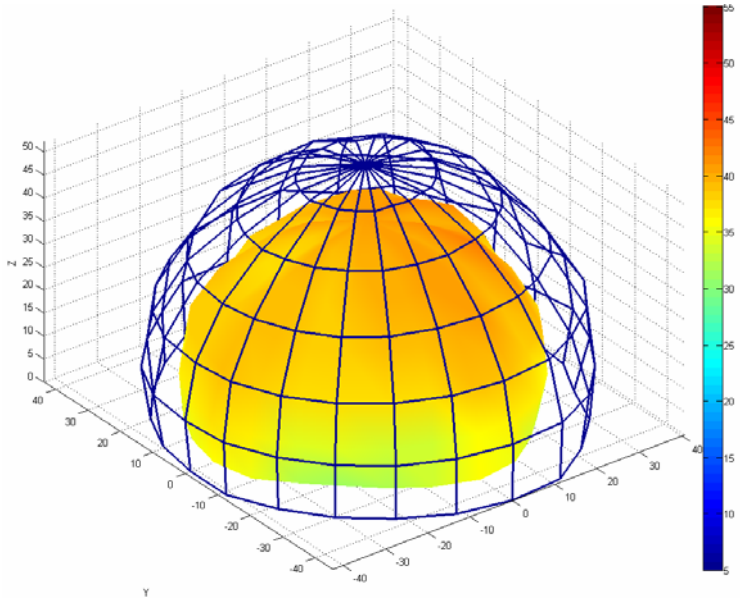

Figure 5.17 Spatial view of BPF narrow band reduction due to multi-channel, decentralized, adaptive feedback control with 200 control taps.

5.7 Predictions and Measured Performance

The above mentioned system was optimized in order to reduce the total group delay to 650 µs. Table 5.1 provides an itemized view of individual group delay contributions.

Source of Delay	**Contribution of Delay**
Acoustical Propagation	Calculated to be 163 µs
DSP Latency	Measured to be 167 µs
Anti-alias Filter	Estimated to be 167 µs
Reconstruction Filter	Estimated to be 34 µs
Microphone Preamplifier Filter	Estimated to be 34 µs
Transducer Response/Other Electronics	Estimated to be 85 µs

Table 5.1. Itemized list of contributors to the total group delay

Once again, Equation 2.3 was used to predict an overall attenuation of 0.5 dB for the system. An overall global attenuation of 0.5 dB was measured. Autocorrelation based control predictions held consistently true for both the loudspeaker and fan primary sources. Figure 2.2 of this thesis predicts that there would be great performance benefits from further reducing group delay. It is expected that a group delay of 400 μs would increase the overall reduction from 0.5 dB to 1.3 dB. A group delay of 300 μs should provide 2.0 dB of reduction; and delays of 250 μs and 200 μs would further increase the expected attenuation to 2.3 dB and 3.0 dB respectively. Since the residual noise after 0.5 dB of overall reduction was rather flat, and based on the shape of the autocorrelation measurement for the fan, it is expected that increased performance due to shortened delay times would be manifested in the form of broadband flow noise reduction.

CHAPTER 6

CONCLUSIONS

It has been demonstrated that an adaptive feedback controller is a viable method for the reduction of axial fan noise, especially in the case where a properly coherent reference signal is unobtainable for feed-forward forms of ANC. It was originally hoped that the results of this research would yield 3.0 dB or more of reduction in the fan noise, however, the attenuation obtained was not insignificant. The feedback controller provided over 10 dB of global reduction of tonal fan noise components as well as some low frequency broadband attenuation. For listeners, this provided a significant reduction in the amount of fan noise that was perceived. The residual, or uncontrolled noise, had a relatively flat frequency response, making it less harsh and annoying to the listener.

The use of autocorrelation measurements has been demonstrated as a reliable tool for prediction of the overall control that can be achieved by feedback ANC. Also, it has been shown that the group delay associated with modern DSP hardware for ANC systems is too long to provide reduction of broadband noise attributed to flow. The lowest group delay achieved in this research, 650 μs, provided for 0.5 dB of overall global fan noise attenuation. A group delay of 300 μs or less would lead to a substantial reduction in the flow noise of an axial cooling fan. While this obstacle was not overcome as a part of this thesis, several methods are suggested in the following three paragraphs to further improve the performance of the feedback controller.

A study of linear prediction as it applies to the correlated portion of axial fan flow noise would be beneficial as future research in the area of feedback ANC for cooling fans. The ability to predict, with some certainty, one or two discrete samples of future

flow noise behavior would overcome some of the effects of the contributions to group delay.

It is also recommended that some non-acoustical sensors be investigated for use as error sensors. A laser vibrometer or an accelerometer might be capable of sensing vibrations due to fan flow. This would provide a more stable and direct estimate of the original disturbance for a feedback ANC approach, or possibly a coherent reference signal for a broadband feed-forward approach.

The analog feedback controller should be revisited and considered, along with feed-forward tonal control, as part of a hybrid controller. With the tonal noise content eliminated, stability is more easily guaranteed in the analog controller and the design of the controller is simplified. The use of an analog controller would eliminate the group delay time due to DSP latency and data conversion. Furthermore, the anti-alias and reconstruction low-pass filters could be replaced with a single low-pass filter. It may be possible to improve the flexibility of the analog controller design if a genetic algorithm was used to produce an analog circuit equivalent for more complex controller transfer functions.

A decentralized controller rather than a centralized controller has been shown to be favorable for this particular multi-channel application of feedback ANC. The effects of source coupling due to mutual impedances between the secondary sources are less significant since the secondary sources are all relatively in phase and the adaptive controller compensates for errors in magnitude estimation. The fact that the decentralized controller does not exactly match the model for far-field predictions based on near-field pressure attenuation is more than compensated for through the increased

number of control filter coefficients made available by the extra simplicity of decentralized control.

Feed-forward and feedback control have been shown to work well together in a hybrid situation. The two systems each contributed their strengths without interfering with the other. Other hybrid controllers should be considered. It is possible that an analog feedback controller could be combined with a digital feed-forward controller in order to maximize the reduction of tonal noise while further reducing the group delay for the system that attenuates broadband noise.

REFERENCES

1. P. Lueg, “Process of Silencing Sound Oscillations” (U.S. Patent No. 2,043,416, 1936).

2. H. F. Olsen and E. G. May, “Electronic Sound Absorber,” J. Acoust. Soc. Am. **25**, 1130-1136 (1953).

3. G. W. Evans and D. Johnson, “Stress and open-office noise,” Journal of Applied Psychology, **85**, 779-783 (2000).

4. G. C. Lauchle, J. R. MacGillivray and D. C. Swanson, “Active control of axial flow fan noise,” J. Acoust. Soc. Am. **101**(1), 341-349 (1997).

5. Kenji Homma, Chris Fuller and Kaleen Xiuting Man, “Broadband active-passive control of small axial fan noise emission,” Proceedings of Noise Con 2003, (2003).

6. D. A. Quinlan, “Application of active control to axial flow fans,” Noise Control Engineering Journal, **39**(3), 95-101 (1992).

7. Kent L. Gee and Scott D. Sommerfeldt, “Application of theoretical modeling to multichannel active control of cooling fan noise,” J. Acoust. Soc. Am. **115**(1), 228-236 (2004).

8. Alan V. Oppenheim and Alan S. Willsky, *Signals & Systems*, **2e**, pp. 94-126, Prentice Hall (1997).

9. Kent L. Gee, “Multi-channel Active Noise Control of Axial Cooling Fan Noise,” Thesis, Brigham Young University, pp. 52-54, (2002).

10. X. Qui, C.H. Hansen, and X. Li, “A Comparison of Near-field Acoustic Error Sensing Strategies for the Active Control of Harmonic Free Field Sound Radiation,” J. Sound Vib. **215**, 81-103 (1998).

11. Stephen Elliott, *"Signal Processing for Active Control,"* Academic Press, 298-299 (2001).

12. Sen M. Kuo, Xuan Kong and Woon S. Gan, "Applications of adaptive feedback active noise control system," IEEE Transactions on Control Systems Technology, **11**(2), 216-220 (2003).

13. Lixi Huang, "Characterizing computer cooling fan noise," J. Acoust. Soc. Am. 114(6), 3189-3200 (2003).

14. B. D. Mugridge and C. L. Morfey, "Sources of Noise in Axial Flow Fans," J. Acoust. Soc. Am. **51**, 1411 (1972).

15. G. F. Franklin, J. D. Powell, and A. Emami-Naeini, *Feedback Control of Dynamic Systems,* **4e**, p. 17, Prentice Hall (2002).

16. G. F. Franklin, J. D. Powell, and A. Emami-Naeini, *Feedback Control of Dynamic Systems*, **4e**, p. 390, Prentice Hall (2002).

17. Alan V. Oppenheim and Alan S. Willsky, *Signals & Systems*, **2e**, p. 64, Prentice Hall (1997).

18. R. C. Dorf, *Modern Control Systems*, **6e**, Addison-Wesley (1990)

19. Alan V. Oppenheim and Alan S. Willsky, *Signals & Systems*, **2e**, pp. 439-510, Prentice Hall (1997).

20. H. Nyquist, "Certain Factors Affecting Telegraph Speed," *Bell Systems Technical Journal*, Vol. 3, 324 (1924).

21. Scott D. Snyder, "Active control – a bigger microprocessor is not always enough," *Noise Control Eng. J.*, **49**(1), (2001).

22. Brian B. Monson and Scott D. Sommerfeldt, “Global active control of tonal noise from small axial cooling fans,” Fifth International Symposium on Active Noise and Vibration Control, (2004).